

Spring 2017

Plasma Striations in Vacuum Chambers

Loren Hamilton Jackson
Bard College

Follow this and additional works at: https://digitalcommons.bard.edu/senproj_s2017



Part of the [Plasma and Beam Physics Commons](#)



This work is licensed under a [Creative Commons Attribution-Noncommercial-No Derivative Works 4.0 License](#).

Recommended Citation

Jackson, Loren Hamilton, "Plasma Striations in Vacuum Chambers" (2017). *Senior Projects Spring 2017*. 349.

https://digitalcommons.bard.edu/senproj_s2017/349

This Open Access work is protected by copyright and/or related rights. It has been provided to you by Bard College's Stevenson Library with permission from the rights-holder(s). You are free to use this work in any way that is permitted by the copyright and related rights. For other uses you need to obtain permission from the rights-holder(s) directly, unless additional rights are indicated by a Creative Commons license in the record and/or on the work itself. For more information, please contact digitalcommons@bard.edu.

Plasma Striations in Vacuum Chambers

A Senior Project submitted to
The Division of Science, Mathematics, and Computing
of
Bard College

by
Loren Jackson

Annandale-on-Hudson, New York
May, 2017

Abstract

Plasma, often referred to as the fourth state of matter, is ionized gas consisting of positive ions and free electrons. Specifically, a glow discharge is a glowing plasma formed by a voltage across a low pressure gas. The area of the glow discharge of interest in this study is the positive column, a relatively long column of pink, glowing plasma, and its bright and dark striated patterns.

The striated positive column resembles pattern phenomena caused by standing pressure waves. These pressure wave patterns are due to the length of the tube in which they are contained. However, in past plasma research, the relation between striations and plasma tube length has been a neglected parameter.

This study investigates how altering the spacing between electrodes, in effect altering the length of the tube, causes a change in the positive column. This parameter is changed by utilizing four tubes of different lengths and a movable cathode. Research was conducted in both air and argon gas.

It is found that changing electrode spacing does not alter the distance between striations, suggesting the analogy between standing pressure waves and the mechanisms of the positive column do not align along this parameter. Yet, a change in electrode spacing does alter the length of the entire positive column, falling along a clear linear relationship. This relationship is used to suggest the minimum spacing needed to achieve a positive column in both air and argon gas.

Contents

Abstract	iii
Dedication	vii
Acknowledgments	ix
1 Introduction	1
2 Brief Overview of Plasma Theory	5
2.1 Kinetic Theory of Gases	5
2.1.1 Conservation of Momentum and Energy	6
2.1.2 Collision Time and Mean Free Path	8
2.2 Ionization and Breakdown Voltage	10
2.2.1 Electron Avalanche	11
2.2.2 Positive and Negative Ions	14
2.3 Ion Diffusion	14
2.3.1 Ambipolar Diffusion	14
2.4 Low Pressure Glow Discharge	17
2.4.1 Conditions for Glow Discharge	17
2.4.2 Aston Dark Space	19
2.4.3 Cathode Glow	19
2.4.4 Cathode Dark Space	20
2.4.5 Negative Glow and Faraday Dark Space	20
2.4.6 Positive Column	20
2.4.7 Anode Glow and Anode Dark Space	20
2.5 Striations and Analysis of the Positive Column	21
2.5.1 Axial Ionization Concentration	23
2.5.2 Striation Shape and Length	24

2.5.3	Moving Striations	27
2.6	Sputtering, Sparking, and Arcing	28
2.6.1	Sputtering	29
2.6.2	Sparking	29
2.6.3	Arcing	30
2.7	Experimental Relationships	31
2.7.1	Pressure and Striation Distance	31
2.7.2	Voltage, Current, and Striation Distance	31
2.7.3	Electrode Shape, Tube Dimensions and Striation Distance	31
3	Plasma Tube Design and Construction	35
3.1	Original Design	35
3.2	Secondary Design	37
3.3	Penultimate Design and Final Configuration	38
4	Exploring Parameter Space of the Glow Discharge	41
4.1	Forming the Plasma	41
4.2	Manipulating Parameter Space of Weak Vacuum Plasma	42
4.2.1	Changing Pressure	42
4.2.2	Voltage and Current	44
4.2.3	Shape of Electrode	44
4.2.4	Type of Gas	45
4.2.5	External Magnetic Field	46
4.2.6	Electrode Spacing and Tube Dimensions	48
5	Data Collection and Analysis	49
5.1	Experimental Set-Up and Measurement Techniques	49
5.2	Data and Analysis	53
5.3	Further Studies	57
	Bibliography	59

Dedication

To my brother, Shelby.

Acknowledgments

I am grateful to have this opportunity to thank the Bard College physics professors for their caring patience and dedication to each of their student's education and wellbeing. Specifically, I would like to thank Paul Cadden-Zimansky, Hal Haggard, and Matt Deady; the extraordinary time they commit to their students is not only enriching but displays a deep level of compassion, unique to these three. Additionally, I would like to thank once more my advisor, Paul Cadden-Zimansky, whose guiding support over the last two semesters played an essential role in my project's completion. Thank you to Richard Murphy for assisting me with kindness and understanding in the construction of my apparatus. And lastly, I am pleased to thank my wonderful friends Grady Nixon, August Dine, Avery Mencher, Tom Moore, Leigh Taylor, Alex Bacon, Peter McCormack, Niall Murphy, Ori Carlin, and Max Meynig for all of whose love and spirit has made my time at Bard College challenging and insightful.

1

Introduction

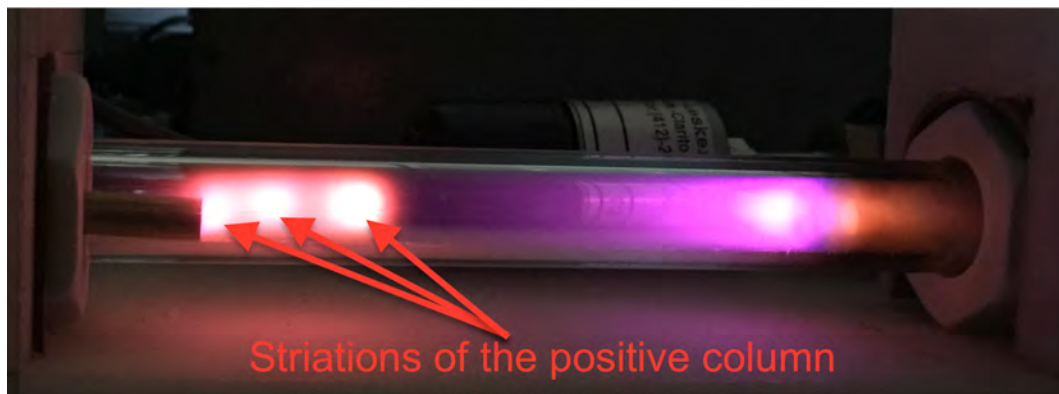


Figure 1.0.1. Image of plasma in vacuum tube.

Often, physicists are not only motivated by empirical considerations. Aesthetic motivations can be seen throughout physical theory. These considerations are simplicity,



Figure 1.0.2. Kundt's tube with dust gathered at the nodes, taken from the University of Michigan Physics Department website [14].

symmetry, beauty, elegance, and order. The Rutherford-Bohr model of the atom evokes order as it reflects the orbits of celestial bodies. This can be seen in Figure 1.0.3. It is simple in its design and spherically symmetric; it helps us understand quantized light emission from an atom through this symmetry, imposing a boundary condition, for the electron orbiting the nucleus must end its journey where it began.

The mathematical invocation of boundary conditions into a system traverses many areas of physics. In a physics student's undergraduate courses boundary conditions are used in classical mechanics, quantum mechanics, thermodynamics, electricity and magnetism, and acoustics to describe many physical phenomena. The points at which a string is held to a guitar determines the tone it can produce, the quantized energy levels of a single electron in an infinite square well are determined by the potentials in which it is contained, and

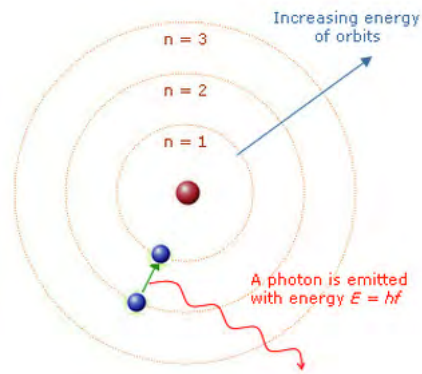


Figure 1.0.3. Rutherford-Bohr model of the atom with n_1 , n_2 , and n_3 electron orbitals, taken from online resource [15].

when any differential equation enters a problem a boundary condition must be used to solve it.

A classical standing wave, also known as a stationary wave, can be viewed as the interference of multiple traveling waves in a medium. Each point on a standing wave has a constant amplitude. The nodes of a standing wave have an amplitude of zero. This means that at the nodes the medium is motionless. Standing waves can be described mathematically using sine or cosine waves.

Standing waves can be visualized using a Kundt's tube. A Kundt's tube consists of a glass tube filled with dust, with a speaker placed at one end of the tube and a moveable piston at the other. A sound wave is sent through the tube with the speaker. The wave reflects off the piston and travels back towards the speaker. A standing wave is achieved in a Kundt's tube when twice the length of the tube is a multiple of tone's wavelength generated by the speaker. The sound wave generated from the speaker and the wave reflecting from the wall align in such a way that the addition of the waves' amplitudes cause nodes with constant position. The dust in the Kundt's tube is vibrated away from positions of high amplitude into the nodes, as is seen in Figure 1.0.2.

The positive column of a glow discharge is displayed in Figure 1.0.1. Within the positive column there are bright and dark areas. These bright and dark areas are known as plasma striations. Plasma striations are visually similar to the dust patterns seen in a Kundt's tube; however, unlike the dust patterns, what causes these patterns in plasma isn't as easily described mathematically. Through analogy, possibly these two phenomena are related by a boundary condition. This paper is a search for what that might be.

Chapter 2 begins with a basic overview of the plasma theory needed to understand what a plasma is and how it forms. This is followed by a more in-depth analysis of the striated positive column presented originally in *Gaseous Conductors* [1] and *Striations* [5]. Next is a collection of empirical relationships between the positive column and certain plasma parameters from past experiments. Chapter 3 discusses the design and construction of the plasma tube used in this study. Chapter 4 initially describes techniques for forming a plasma. The following section details an exploration of the plasma parameters, states qualitative results from these explorations, and argues for an experimental focus on the effect of electrode spacing on both striation length and positive column length. To finish, Chapter 5 outlines the measurement techniques and setup of the experiment, presents an analysis of the collected data, and concludes with motivations for two additional experimental avenues to explore.

2

Brief Overview of Plasma Theory

The plasma considered in this investigation is the product of electric fields and low pressures, maintained inside tubes with gas between two high-voltage electrodes. Plasma is ionized gas, considered the fourth state of matter, consisting of free positive ions and electrons, undergoing a constant process of recombination and ionization. We encounter plasmas everyday, from neon lamps and fluorescent lighting, to static shocks during the winter and lightning during rain storms. Our sun is a plasma, ionized by heat due to nuclear fusion. In simplest of terms, plasma is glowing gas, as seen in Figure 1.0.1.

This chapter is an overview of the basic physical theory needed to understand the phenomena of interest in this study. The theory detailed in the sections to follow is a compilation of facts and models found in textbooks *Gaseous Conductors* [1], *Plasma Physics and Engineering* [2], and *Conduction of Electricity Through Gases* [9], as well as a number of early papers in the study of plasma, which can be found in the bibliography.

2.1 Kinetic Theory of Gases

The kinetic theory of gas is predicated on an idealized picture of gas. In this theory, gas consists of a large number of tiny, spherical particles, randomly moving about and colliding with one another. The molecules are subject to Newton's Laws. The process in which these

spherical bodies collide can be explained through the classical momentum-conservation law.

2.1.1 Conservation of Momentum and Energy

The one-dimensional law of conservation of momentum between two masses m_1 and m_2 is

$$m_1 v_{1i} + m_2 v_{2i} = m_1 v_{1f} + m_2 v_{2f}. \quad (2.1.1)$$

Here, v_{1i} and v_{2i} are the initial velocities of m_1 and m_2 respectively. Likewise, v_{1f} and v_{2f} are the final velocities of the two masses.

An elastic collision is a collision in which momentum and kinetic energy are conserved; there is no net loss in the kinetic energy of the system. Consider the elastic collision between m_1 moving at velocity v_1 with a mass at rest, m_2 . The conservation of momentum relationship for this is,

$$m_1 v_{1i} = m_1 v_{1f} + m_2 v_{2f}. \quad (2.1.2)$$

The law of conservation of energy for particles m_1 and m_2 is

$$\frac{m_1 v_{1i}^2}{2} = \frac{m_1 v_{1f}^2}{2} + \frac{m_2 v_{2f}^2}{2}. \quad (2.1.3)$$

By solving for v_{1i} in Eq. 2.1.2 and substituting it into eq. 2.1.3

$$m_2 v_{2f}^2 + \frac{m_2^2 v_{2f}^2}{m_1} - 2m_2 v_{1i} v_{2f} = 0, \quad (2.1.4)$$

and solving for v_{2f} in Eq. 2.1.4 v_{2f}

$$v_{2f} = \frac{2m_1 v_{1i}}{m_1 + m_2}, \quad (2.1.5)$$

we find the final velocity of the impacting particle m_1 is

$$v_{1f} = \frac{(m_1 - m_2)v_{1i}}{m_1 + m_2}. \quad (2.1.6)$$

If $m_1 > m_2$, m_1 continues moving in the same direction but with a different velocity.

If $m_1 < m_2$, like in the case of an electron colliding with a wall, the direction of m_1 is reversed.

In order to understand gas ionization the theory must account for inelastic collisions. Inelastic collisions, unlike elastic collisions described above, change the internal energy of the colliding particles. This change in internal energy is required for ionization to occur. A similar process as the one detailed above can be used to find the change in internal energy cause by an inelastic collision.

Consider the two masses from before, m_1 and m_2 , and the change in internal energy U . The law of conservation of energy tells us, expanding on the thought in Eq. 2.1.3,

$$\frac{m_1 v_{1i}^2}{2} = \frac{m_1 v_{1f}^2}{2} + \frac{m_2 v_{2f}^2}{2} + U. \quad (2.1.7)$$

Conservation of momentum is the same as it was above in Eq. 2.1.2. Solving for v_{2f} in eq. 2.1.2,

$$\frac{m_1}{m_1}(v_{1i} - v_{1f}) = v_{2f}, \quad (2.1.8)$$

and substituting v_{2f} from Eq. 2.1.8 into eq. 2.1.7, we find,

$$m_1 v_{1i}^2 = m_1 v_{1f}^2 + m_2 \left(\frac{m_1 v_{1i} - m_1 v_{1f}}{m_2} \right)^2 + 2U. \quad (2.1.9)$$

The maximum change in internal energy is found by differentiating Eq. 2.1.9 with respect to v_{1f} and setting it equal to zero.

$$\begin{aligned} \frac{dU}{dv_{1f}} &= \frac{m_1^2 v_{1i}}{m_2} - \frac{m_1^2 (m_1 + m_2) v_{1f}}{m_2} = 0 \\ \frac{m_1^2 v_{1i}}{m_2} &= \frac{m_1^2 (m_1 + m_2) v_{1f}}{m_2} \\ v_{1f} &= \frac{m_1 v_{1i}}{m_1 + m_2}. \end{aligned} \quad (2.1.10)$$

Eq. 2.1.10 is the value of v_{1f} when U is maximized. Substituting this value into Eq. 2.1.9 results in the maximum change in internal energy in an inelastic collision between a moving and stationary particle,

$$U_{max} = \frac{m_2}{m_1 + m_2} \frac{m_1 v_{1i}^2}{2}. \quad (2.1.11)$$

This gives a basic understanding of the maximum change in internal energy during an inelastic collision of an electron and atom of gas.

It is known that during these collisions the internal energy of a molecule can change only in discrete amounts of U_{max} . Atoms can only exist in specific quantum states which correspond to a specific energy. The internal energy of an atom depends on the energy of the electrons that orbit the nucleus. Electrons orbiting a nucleus are restricted to certain energy levels and can move only from one allowed energy level to another. The quantization of electron energy levels is due to the wave nature of electrons and boundary conditions imposed the Coulomb potential of the nucleus. Like a string bound at both ends, only being able to oscillate at specific frequencies, the wavelength of an electron needs to satisfy the boundary conditions determined by the nucleus of the atom. This is why the electrons of an atom can only occupy certain energy levels, and the internal energy of a molecule can only change in discrete amounts during a collisions.

In order to understand the ionization process that causes the formation of plasma one must consider the frequency in which these inelastic collisions take place.

2.1.2 Collision Time and Mean Free Path

In plasma, electrons collide with atoms of the gas inside the plasma tube. The collisions begin with an emitted electron from the cathode. The cathode is the negatively charged electrode within the tube. The second electrode, known as the anode, is positively charged and at a high voltage relative to the cathode. The collision time and mean free path of a particle is derived below and can be found of page 463 *Fundamentals of Statistical and Thermal Physics* [3]. The collision time of a particle is the average amount of time before it suffers a collision. The mean free path is the average distance particles of a certain species in a certain environment travel before suffering a collision.

Let $P(t)$ be the probability that a molecule survives a time t without suffering a collision. Before the emission of an electron from the cathode,

$$P(0) = 1. \quad (2.1.12)$$

$P(t)$ decreases as t increases.

$$P(t) \rightarrow 0, t \rightarrow \infty. \quad (2.1.13)$$

The probability a molecule suffers a collision between t and $t + dt$ is given by $w dt$. Where w is the probability of a collision per unit time. This is known as the collision rate which depends on velocity: $w(v)$. The probability a molecule does not suffer a collision between t and $(t + dt)$ is given by $(1 - w dt)$ so that $P(t + dt)$ and $P(t)$ are related by,

$$P(t + dt) = P(t)(1 - w dt) \quad (2.1.14)$$

$$\frac{1}{P} \frac{dP}{dt} = -w. \quad (2.1.15)$$

Multiplying both sides by P , we have the differential equation

$$\frac{dP}{dt} = -wP \quad (2.1.16)$$

with solutions

$$P = Ce^{-wt}. \quad (2.1.17)$$

C is a constant of integration. The normalization condition is found by taking the time derivative of 2.1.17,

$$P(t)dt = -Ce^{-wt}w dt, \quad (2.1.18)$$

and integrating the result across all possible values of t ,

$$\int_0^\infty P(t) dt = 1. \quad (2.1.19)$$

So, $C = w$.

Let $\tau \equiv \bar{t}$. τ is found by integrating the product of the probability, $P(t)$, and the time variable, t , over all values of t to find the mean value of t ,

$$\tau = \bar{t} = \int_0^\infty P(t)t dt. \quad (2.1.20)$$

τ is the mean time between collisions. It is known as the *collision time* or the *relaxation time* of the molecule. We can find τ in terms of w by making a substitution utilizing Eq. 2.1.18 in Eq. 2.1.20,

$$\tau = \int_0^{\infty} e^{-wt} w dt \quad (2.1.21)$$

With a change of variables, letting $y = wt$ and $dy = w dt$, Eq. 2.1.21 becomes,

$$\tau = \frac{1}{w} \int_0^{\infty} e^{-y} y dy. \quad (2.1.22)$$

The integral of Eq. 2.1.22 equals one and $\tau = \frac{1}{w}$. therefore, the collision time depends on the velocity of the molecule because the collision rate depends on v . The mean free path of a particle, often abbreviated as m.f.p., is the average distance traveled between collisions. The mean free path, L , is described by the product of the collision time and the average velocity; therefore, the mean distance traveled by a molecule is,

$$L(\bar{v}) = \bar{v} \tau(\bar{v}). \quad (2.1.23)$$

2.2 Ionization and Breakdown Voltage

The breakdown voltage is the minimum voltage required to cause an insulator to become conductive. At the breakdown voltage, ionization of the gas will cause an electron avalanche. An electron avalanche is the process of electrons accelerating through a medium due to a high electric field; the electrons cause ionization through collisions with atoms, resulting in an increase of electrons that also accelerate through the medium, causing ionization, and ultimately resulting in a chain reaction of electron collision ionization of the gas.

Breakdown voltage depends upon the pressure of the tube and the distance between anode and cathode. At the breakdown voltage, electrons from the cathode are given enough energy to ionize the neutral gas within the tube.

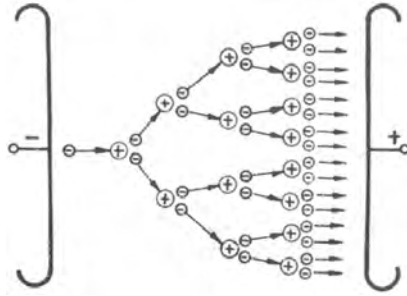


Figure 2.2.1. Electron Avalanche Illustration from *Gaseous Dielectrics* [10]

2.2.1 Electron Avalanche

Plasma is ionized gas consisting of positive ions and electrons. For the ignition of a plasma, ionization is required. The most simple and common cause of ionization in plasma is from the impact between electrons and atoms. When a cold cathode emits electrons into a gas, the electrons emitted have a certain probability of colliding with atoms of the gas. The previous Section 2.1.2 details the probability that a molecule survives a time t without suffering a collision. When a collision occurs, and if the electron has enough energy, it may knock an electron free, resulting in two free electrons and one positive ion. These two

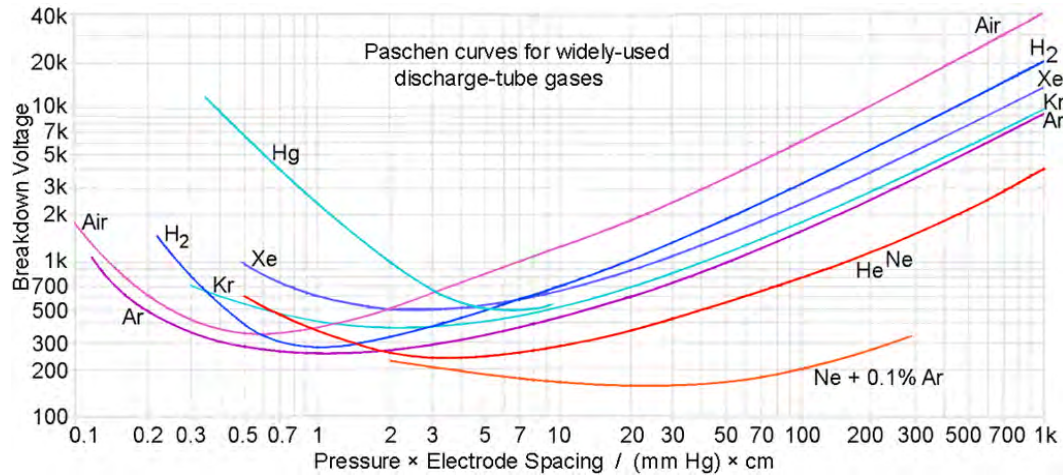


Figure 2.2.2. Curves Relating Breakdown Voltage to Pressure and Electrode Spacing of Plasma Tube. Figure found in *Gas Tube Design* [11].

electrons continue to strike atoms, releasing more free electrons, leaving behind positive ions. This chain reaction of electron collisions, resulting in a flood of electrons free to move from cathode to anode, is called the electron avalanche. An illustration of an electron avalanche occurring between anode and cathode is given by Figure 2.2.1.

The ionization process of argon gas, $e + Ar = Ar^+ + e + e$, is given by Figure 2.2.3. The energy required of the incident electron to cause this reaction is $15.8eV$. If the voltage across a plasma tube is lower than the voltage needed for ionization, the plasma will not ignite. In fact, the energy of the incident electron must exceed the lowest energy needed for ionization so that the valence electron is endowed with enough energy to ionize another atom of the gas for an electron avalanche to occur.

Figure 2.2.1 gives a clear illustration of how breakdown voltage depends on pressure and electrode spacing. At high pressure, the breakdown voltage is high. There appears to be a

TABLE 2.1

Ionization Energies for Different Atoms, Radicals, and Molecules

Reaction Process	I (eV)	Reaction Process	I (eV)
$e + N_2 = N_2^+ + e + e$	15.6	$e + O_2 = O_2^+ + e + e$	12.2
$e + CO_2 = CO_2^+ + e + e$	13.8	$e + CO = CO^+ + e + e$	14.0
$e + H_2 = H_2^+ + e + e$	15.4	$e + OH = OH^+ + e + e$	13.2
$e + H_2O = H_2O^+ + e + e$	12.6	$e + F_2 = F_2^+ + e + e$	15.7
$e + H_2S = H_2S^+ + e + e$	10.5	$e + HS = HS^+ + e + e$	10.4
$e + SF_6 = SF_6^+ + e + e$	16.2	$e + SiH_4 = SiH_4^+ + e + e$	11.4
$e + UF_6 = UF_6^+ + e + e$	14.1	$e + Cs_2 = Cs_2^+ + e + e$	3.5
$e + Li_2 = Li_2^+ + e + e$	4.9	$e + K_2 = K_2^+ + e + e$	3.6
$e + CH_4 = CH_4^+ + e + e$	12.7	$e + C_2H_2 = C_2H_2^+ + e + e$	11.4
$e + CF_4 = CF_4^+ + e + e$	15.6	$e + CCl_4 = CCl_4^+ + e + e$	11.5
$e + H = H^+ + e + e$	13.6	$e + O = O^+ + e + e$	13.6
$e + He = He^+ + e + e$	24.6	$e + Ne = Ne^+ + e + e$	21.6
$e + Ar = Ar^+ + e + e$	15.8	$e + Kr = Kr^+ + e + e$	14.0
$e + Xe = Xe^+ + e + e$	12.1	$e + N = N^+ + e + e$	14.5
$e + C_2H_5OH = e + C_2H_5OH^+ + 2e$	0.5	$e + CH_3COOH = e + CH_3COOH^+ + 2e$	0.4
$e + C_6H_5OH = e + C_6H_5OH^+ + 2e$	8.5	Naphthaldehyde	7.7
$e + (C_2H_5)_2Cr = e + (C_2H_5)_2Cr^+ + 2e$	5.5	4-Methyl-phenylene-diamine	6.2

Figure 2.2.3. Table 2.1 from *Plasma Physics and Engineering* [2].

screening effect, like that of a dielectric, at high pressure. A dielectric is a non-conductive medium which can become polarized by an electric field. Polarization is the process of positive charges in a material shifting due to the applied electric field; positive charges align in the direction of the electric field while negative charges align in the opposite direction of the electric field. Polarization causes an electric field, due to the displaced charges in the medium, in the opposite direction of the applied electric field. The electric field resulting from polarization dampens the applied electric field, known as screening.

At low pressure, the breakdown voltage required is also maximized. In this case, there is a smaller number of atoms present in the gas, making it more difficult for the chain reaction to occur, resulting in a higher energy needed to form a plasma.

2.2.2 Positive and Negative Ions

The positive ions of the plasma in which this study deals, because the plasma in question is relatively cold, are opposite and equal to the charge of the electrons. The ionization process results in equal quantity of positive ions and electrons, resulting in a neutral plasma. According to *Plasma Physics and Engineering* [2], due to their large mass with respect to electrons, positive ions remain relatively stationary.

2.3 Ion Diffusion

Diffusion is the spreading and mixing of molecules due to their kinetic energy. After a gas is ionized by an applied voltage, there is a diffusion of the positive and negative ions. In the case of one type of gas, the diffusion rate, M , of the gas molecule depends on its average velocity, its mass, and the dimensions of the medium through which the molecule is diffusing,

$$M = K \sqrt{\frac{\bar{c}}{m}}. \quad (2.3.1)$$

In the relationship above, K is a constant dependent on the cross-sectional area through which the molecule diffuses, \bar{c} is its average velocity, and m is its mass. The ratio of diffusion rates of two species, known as relative diffusion, is equal to the square root of the quotient of the two species' masses. An example of relative diffusion rate is ambipolar diffusion.

2.3.1 Ambipolar Diffusion

The diffusion of electrons and positive ions of a plasma is much different than that of the gas molecules from which the plasma forms. The mass and velocity of electrons and positive ions are both very different from one another and from the atoms of the gas in which they diffuse. According to *Gaseous Conductors* [1], the diffusion relationship between one type of gas with respect to another is,

$$D_{12} = \frac{n_1 L_2 \bar{c}_2 + n_2 L_1 \bar{c}_1}{3(n_1 + n_2)}. \quad (2.3.2)$$

D_{12} is the coefficient of diffusion of the first type of gas into the second type of gas, n is the concentration of each type of particle, L is the mean free path of each type of particle, and \bar{c} is the average velocity of each type of particle. The mean free path for particles of type 1 colliding with particles of type 2, excluding collisions between like particles, is derived in *Gaseous Conductors* [1] as,

$$L_1 = \frac{1}{\pi n_2 r_{12}^2 [1 + (C_2^2/C_1^2)^{1/2}]} \quad (2.3.3)$$

Here, r_{12} is the sum of the radii of the two gasses. n_2 is the number of particles of type 2 per cubic centimeter. C_1 and C_2 are the effective velocities for each type. Letting $n = (n_1 + n_2)$ and value for L_1 and L_2 are substituted into Eq. 2.3.2 on the basis of Eq. 2.3.3, the coefficient D_{12} becomes,

$$D_{12} = \frac{1}{3n\pi r_{12}^2} \left(\frac{\bar{c}_1 C_1 + \bar{c}_2 C_2}{(C_1^2 + C_2^2)^{1/2}} \right). \quad (2.3.4)$$

This diffusion coefficient ignores the impact of particles of the same kind because those impacts on average do not affect diffusion. The diffusion coefficient of negative ions is greater than the diffusion coefficient of positive ions. This is because positive ions are much more massive than negative ions, so collisions with electrons have little effect on their movement. This difference in diffusion coefficients causes an excess of negative ions at the boundary of the ionized region.

The diffusion coefficient of positive and negative ions, also known as the ambipolar diffusion coefficient, can be found using the process above. In this specific case, n^+ and n^- , corresponding to n_1 and n_2 in the equations above, are the number of positive and negative ions per cubic centimeter. The velocity of the positive ions is given in *Gaseous Conductors* [1] as,

$$v^+ = \frac{-D^+}{n^+} \frac{dn^+}{dx} + K^+ E. \quad (2.3.5)$$

$\frac{dn^+}{dx}$ is the concentration gradient of positive ions and E is the electric field. The gradient and electric field add to the diffusion of the positive ions by applied force. K^+ is the electrical mobility of the positive ions. Electrical mobility describes the ability for a charged

particle to move through a medium due to an electric field. Mobility is defined as,

$$K = \frac{q}{mv_m}. \quad (2.3.6)$$

Here, q is the charge of the particle, m is the mass, and v_m is the momentum transfer collision frequency. The higher the mobility for a particle, the easier it moves through a medium. For example, electrons are highly mobile in comparison to positive ions within a plasma because, since the charge of each is equal in magnitude, the mass of the electrons is much smaller than the mass of the positive ions.

The velocity of the negative ions is similar in form to that of the positive ions except the sign on the mobility and electric field component is switched,

$$v^- = \frac{-D^-}{n^-} \frac{dn^-}{dx} - K^- E. \quad (2.3.7)$$

According to *Gaseous Conductors* [1], the diffusion of the electrons leaves a net positive charge at the center of the tube. This positive charge creates an electric field that slows down electron diffusion to the walls, resulting in an average velocity of diffusion which is equal to the negative and positive ion velocities.

Eliminating E from Eqs. 2.3.5 and 2.3.7 and allowing $n^+ = n^- = n$, $dn^+/dx = dn^-/dx = dn/dx$, and $v^+ = v^- = \bar{v}$ the average diffusion velocity is,

$$\bar{v} = -\frac{D^+K^- + D^-K^+}{n(K^+ + K^-)} \frac{dn}{dx}. \quad (2.3.8)$$

Therefore, the ambipolar diffusion coefficient, which is the average diffusion coefficient of the positive and negative ions, is,

$$D_a = \frac{D^+K^- + D^-K^+}{K^+ + K^-}. \quad (2.3.9)$$

The ambipolar diffusion coefficient is important in understanding the shape of striations of the positive column (see section 2.5.2).

2.4 Low Pressure Glow Discharge

A glow discharge is achieved with a low current, high voltage device, such as the one used in this study. In this case, discharge refers to the movement of electrons through an insulator, like gas, after it is made conductive through ionization. In the context of plasmas, discharge refers to ionization between a gap. Glow discharge specifically refers to ionization between a gap that is luminous. In low pressure discharge, all areas between electrode and anode are emitting light. Dark spaces of the discharge are only dark in comparison to the layers in which they are adjacent.

2.4.1 Conditions for Glow Discharge

The required voltage to ignite a glow discharge is primarily determined by the gas, gas pressure, and orientation and shape of the electrodes. This DC voltage V can be determined in a circuit connected in series with the vacuum tube and a resistor of resistance R , by equations 2.4.1 and 2.4.2 below.

$$V_d = V_b - iR \quad (2.4.1)$$

$$V_b - iR - V_d = \Delta V_d \quad (2.4.2)$$

Here, V_d is the voltage across the plasma which is known as the discharge voltage, V_b is the applied voltage, and i is the current passing through the resistor R . Considering Eq. 2.4.2 if ΔV_d is greater than or less than zero, the current i must increase or decrease respectively. Let's allow the change in discharge voltage to be negative, then

$$\Delta V_d < 0 \implies iR + V_d > V_b.$$

If the sum of the resistance drop and the discharge voltage is greater than the applied voltage, the current must decrease to satisfy Eq. 2.4.1. Likewise,

$$\Delta V_d > 0 \implies iR + V_d < V_b.$$

In this case, to satisfy Eq. 2.4.1, the current must increase. These conditions lead to the mathematical condition of stability for glow discharge as

$$\frac{dV_d}{di} + R > 0. \quad (2.4.3)$$

de/di is the change in discharge voltage with respect to current and can be understood as a resistance which maintains the stability of the glow discharge.

Information about the regions described in the following sections, 2.4.2 - 2.4.7, can be found in *Gaseous Conductors* [1] and *Plasma Physics and Engineering* [2].

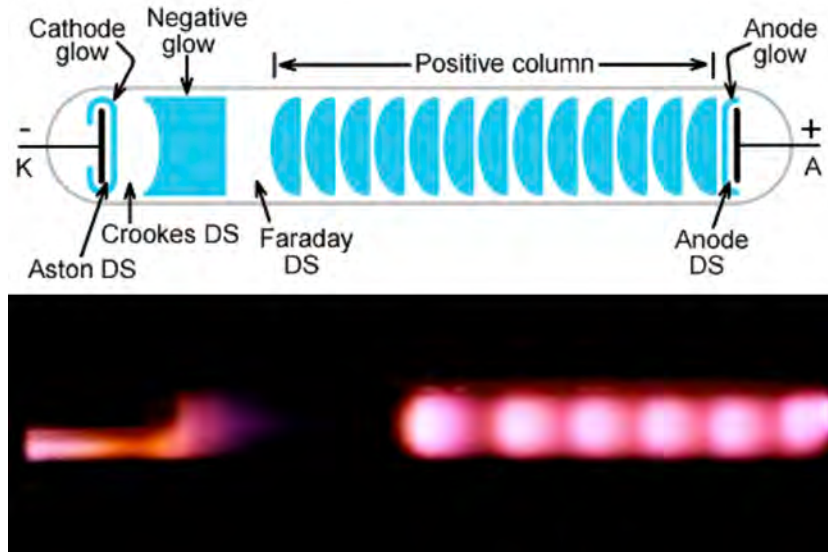


Figure 2.4.1. Illustration of Positive Glow Areas, Found in *Gas Discharge Tubes* [12], and a glow discharge formed at 300 mTorr and 500 V in air.

Figure 2.4.1 shows a schematic of the glow discharge regions. A description of those regions is presented below. Figure 2.4.2 gives (a) structure of the glow discharge, (b) light emission intensity, (c) voltage, (d) electric field, (e) current density, (f) electron and ion density, and (g) charge density for each region.

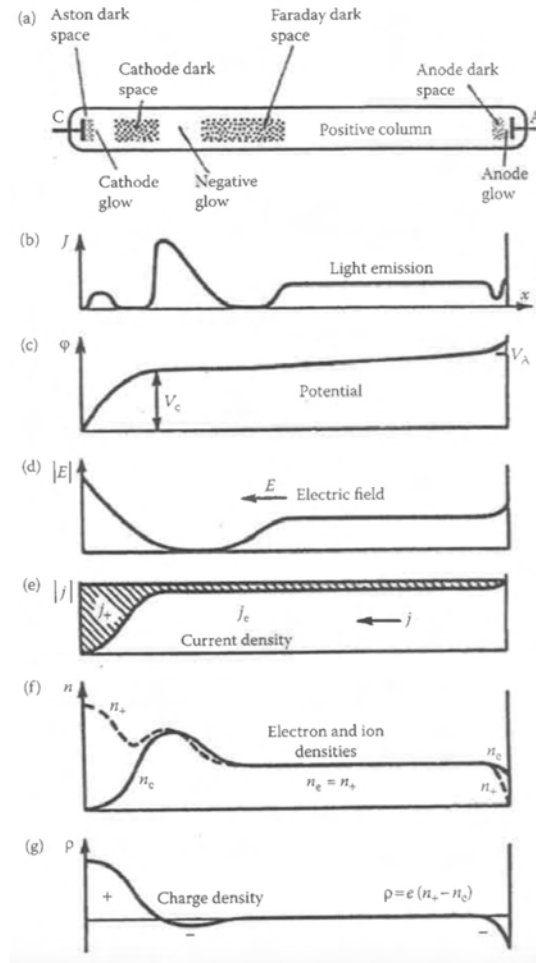


Figure 2.4.2. Physical parameters distribution in a glow discharge, taken from *Plasma Physics and Engineering* [2]. Key: (a) structure of the glow discharge; (b) light emission intensity; (c) voltage; (d) electric field; (e) current density; (f) electron and ion density; (g) charge density

2.4.2 Aston Dark Space

The Aston dark space is located directly in front of the cathode. In this area there is a small potential, high electric field, and low current density. This space is very thin and makes up little of the cathode layer.

2.4.3 Cathode Glow

The cathode glow is located next to the Aston dark space. It's size depends on the type of gas and the pressure. Similar to the Aston dark space, this area is of low voltage, high

electric field, and low charge density. Often the cathode glow hides the Aston dark space with the bright light it emits.

2.4.4 Cathode Dark Space

The cathode dark space follows after the cathode glow. This area is also known as the Crookes dark space or the Hittorf dark space. Likewise, this area is also of low voltage, high electric field, and low charge density.

2.4.5 Negative Glow and Faraday Dark Space

The negative glow and the Faraday dark space are not sharply distinct. The negative glow gradually decreases in light intensity as it transitions into the Faraday dark space. This area has a net charge density of zero and a high current density. Ionization and recombination occurs in these dark spaces and are only dark in comparison to the positive column and cathode glow. Here, ionization by electron collision is not as prominent as ionization due to photon absorption from the glowing regions.

2.4.6 Positive Column

The positive column is the longest region of the tube. It glows brightly pink, following the Faraday dark space. In the positive column, many parameters of the glow discharge are constant. The net charge density, electric field, and current density are all uniform. The gas temperature of the positive column is typically under 100°C which motivates only considering electron collisions as the main form of ionization instead of thermal ionization. In early experiments into glow discharge, according to *Gaseous Conductors*, the positive column was assumed to be five tube diameters shorter than the electrode spacing [1].

Analysis of the positive column can be found in the following section 2.5.

2.4.7 Anode Glow and Anode Dark Space

The anode glow is a bright region which emits light in front of the anode, but is separated from the anode by the anode dark space. It is often hard to see the anode glow and anode

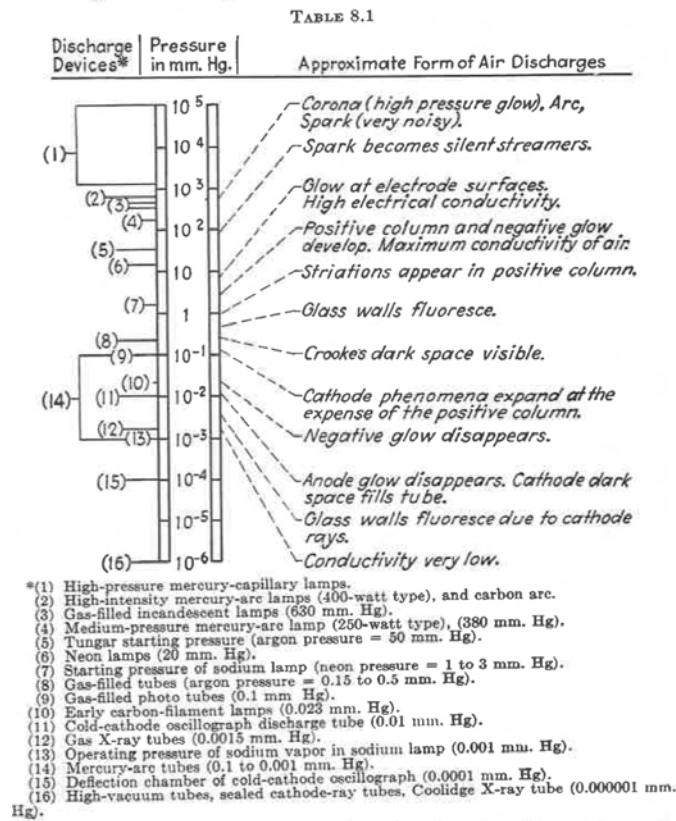
dark space due to the glow of the positive column. There is a negative charge density directly in front of the anode. The anode, which is at high voltage, cannot release positive ions in the way the cathode can release electrons. Positive ions accelerate away from the anode. The acceleration of positive ions away from the anode and the negative charge density near it results in a voltage drop. The distance which this voltage drop spans is small and is not represented in (c) of Figure 2.4.2. The potential drop in this region is of the order of the ionization potential. In this region, electrons produce positive ions which diffuse axially towards the walls of the plasma tube.

2.5 Striations and Analysis of the Positive Column

Striations are seen as bright areas of the positive column, perpendicular to the direction of the current flow. These bright areas are separated by similarly shaped dark areas. The dark spots glow as well and are only dark in contrast to the bright ones. The bright striations of the positive column are not sharply defined but gradually taper off in intensity into the dark regions.

The positive column only appears at a certain low pressure and a certain high voltage. As pressure is decreased with constant voltage, the plasma phenomena seen is, according to Figure 2.5.1: arcing accompanied by a loud sound, silent arcing, glowing at the surface of each electrode, the first instance of the positive column, striations of the positive column, walls of the vacuum tube fluoresce, Crookes dark space is visible, negative glow disappears, anode glow disappears, the cathode dark space fills the vacuum tube, and finally cathode rays appear.

The brightest regions of the plasma are due to a higher level of recombinations of the negative and positive ions within the tube. The positive column is understood to be a conducting path for the current which flows through the tube. The strength of the electric field is highest next to the cathode. This high electric field is responsible for the cathode

Figure 2.5.1. Table 8.1 from *Gaseous Conductors* [1].

dark space. One can see that where there is not a glowing discharge, we either have a greater potential drop or a very low pressure.

What is interesting about the positive column is that it contains a regular pattern of bright and dark filaments while maintaining a nearly constant voltage gradient, net charge density, net positive charge density, net negative charge density, and electron current density according to *Gaseous Conductors* [1].

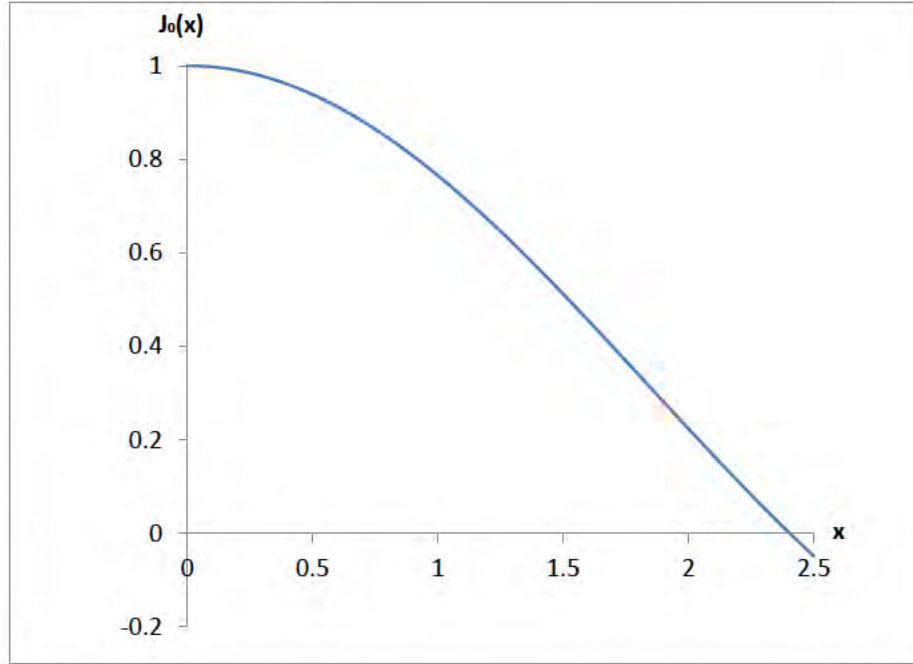


Figure 2.5.2. Zeroth order Bessel function plot [1].

2.5.1 Axial Ionization Concentration

The positive and negative ion concentration, n^+ and n^- , of striations can be described by the solution to the differential equation given in *Gaseous Conductors* [1],

$$\frac{d^2n}{dr^2} + \frac{1}{r} \frac{dn}{dr} + \frac{z}{D_a} n = 0. \quad (2.5.1)$$

Here, $n^+ = n^- = n$, z is the number of ionizing collisions per second, and r is the radial component of the plasma. The solution to Eq. 2.5.1 is,

$$n_r = n_0 J_0(x) = n_0 J_0\left(r \sqrt{\frac{z}{D_a}}\right). \quad (2.5.2)$$

n_0 is the concentration of ions along the axis of the positive column $r = 0$ and x is the substitution $r = \sqrt{\frac{D_a}{z}} x$. $J_0(x)$ is the zeroth order Bessel function. This function is plotted in Figure 2.5.2. The plot shows the first zero of the Bessel function occurs at $x = 2.405$, which corresponds to $r = R$ [1]. This means that at R , the radius of the tube, $J_0(x)$ is

zero. If $J_0(x)$ is zero, then n_r is zero as well, meaning there is no positive and negative ion concentration at the walls. However, this is not the case for there must be a net charge at the walls to form the equipotential lines described. This contradiction is explained by Nedospasov's jump discontinuity outlined in Section 2.5.2. As the radius decreases towards the axis of the column, the ion concentration increases resulting in an increase of recombinations occurring toward the center of the column.

2.5.2 Striation Shape and Length

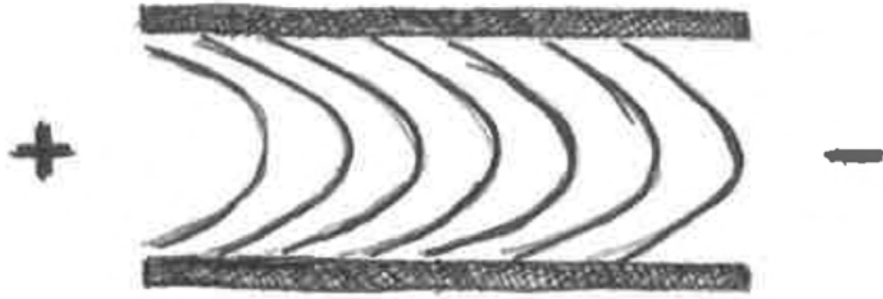


Figure 2.5.3. Illustration of equipotential lines from *Gaseous Conductors* [1].

Striations are dependent upon the fact that ionization and recombination occurs only within the limits of the striations [5]. The recombinations taking place is the cause for photon emission. Where recombination and ionization takes place determines the shape of the striation. Striations of the positive column are somewhat oval shaped. On the cathode end of each striation, they curve outward. Striations are nearly perpendicular to

the length of the plasma tube on their anode edge. The shape of striations is a result of charge depositing on the wall of the plasma tube.

According to *Gaseous Conductors* [1], in the glow discharge, the positive ion temperature is much lower than the electron temperature. This causes the walls of the plasma tube to become negatively charged. The negatively charged walls cause an electric field through the tube that is not uniformly parallel to the length of the tube. The equipotential lines of the plasma i.e, lines of constant potential, are bowed towards the cathode. Equipotential lines are lines of constant potential. An illustration of these equipotential lines is given by Figure. 2.5.3. The curved edges of striations in the positive column follow these equipotential lines. The positive ion and electron diffusion to the walls of the plasma tube is determined by the ambipolar diffusion coefficient, derived in Section 2.3.1,

$$D_a = \frac{D^+ K^- + D^- K^+}{K^+ + K^-}. \quad (2.5.3)$$

Here, K^+ and K^- are the mobility constants for the positive and negative ions. D^+ and D^- are the diffusion coefficients for the positive and negative ions. Ambipolar diffusion refers to the diffusion of both positive and negative ions. The negative ion diffusion coefficient is greater than the positive diffusion coefficient in plasma, resulting in a negative charge on the glass of the plasma tube. This negative charge buildup leaves a net positive charge at the center of the tube, resulting in an electric field pointing from the center of the tube to the walls in addition to the field maintained by the anode and cathode.

This electric field acts against the electron diffusion to the walls while increasing the diffusion of the positive ions. According to *Striations* [5], the ionization on the cathode end of the striations is intensified by, and on the anode side the electric diffusion field is opposite to, the applied field. Nedospasov gives the longitudinal electric field as

$$E = \frac{j}{e_0 b_e n} - \frac{D_e \delta n}{b_e n}. \quad (2.5.4)$$

Here, j is the current density, b_e is the mobility of the electrons, n is the number of electrons, and δn is the local increase of electrons. The length of stationary striations can

be found by considering moving striations with a velocity v . Only considering ionization taking place at the cathode side boundary of the striation and recombination taking place on the walls of the tube, Nedospasov states the electron distribution n is given by,

$$D_a n''_\xi + v n'_\xi - \frac{n}{\tau} = 0. \quad (2.5.5)$$

This is a second order differential equation in a reference frame moving with the striations at velocity v . ξ is the change from the lab frame to the moving reference frame, defined as $\xi = z - vt$, and τ is the characteristic time scale of this process, defined as $\tau = \frac{a^2}{\beta^2 D_a}$. The axis of the tube is in the z direction which is oriented at the center of the tube. The positive z direction points from the anode to the cathode. Here, a is the diameter of the plasma tube and β is the eigenvalue of the Bessel function $J_0(\frac{\beta r}{a})$ which describes the radial propagation of density of the striated positive column. (*Note: The radial propagation of ion density is also described using a Bessel function in Gaseous Conductors [1] and is referred to in Section 2.5.1 with Eq. 2.5.1.*)

The eigenvalue, β , of Eq. 2.5.2 is determined by the radius of the positive column. The concentration of ions decreases exponentially in the radial direction. At the walls of the tube, according to Figure 2.5.2, the ion concentration is zero. Nedospasov states however that at this boundary there is a potential jump which generates a new region of high ionization and is the beginning of the next striation. Therefore, striation shape can be understood through the ion concentration analysis in Section 2.5.1.

The solution to Eq. 2.5.5 is

$$n \sim n_0^{-\frac{|\xi|}{2D_a}(v_1-v)}, \quad (2.5.6)$$

$$v_1 = \sqrt{v^2 + \frac{4D_a}{\tau}}. \quad (2.5.7)$$

Nedospasov gives that from Eq. 2.5.4, Eq. 2.5.6, and Eq. 2.5.7 the length of moving striations is approximated at

$$l \approx \frac{(v_1 + v)a^2}{2\beta^2 D_a} \ln \left[1 + \frac{D_e(1 - \frac{v}{v_1})I}{D_a(1 + \frac{v}{v_1})i} \right]. \quad (2.5.8)$$

Here, I is the total recombination current to the walls within a striation, i is the discharge current, and D_e is the electron diffusion coefficient. The length of stationary striations can be found by letting $v = 0$, which results in $v_1 = 2\sqrt{\frac{D_a}{\tau}}$. Plugging v and v_1 into Eq. 2.5.8, the length of the stationary striation is found to be,

$$l = \frac{a}{\beta} \ln \left[1 + \frac{D_e I}{D_a i} \right]. \quad (2.5.9)$$

2.5.3 Moving Striations

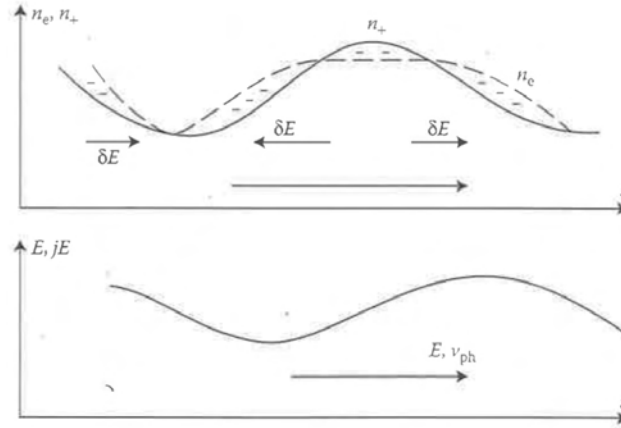


Figure 2.5.4. Propagation of striations illustration, taken from *Plasma Physics and Engineering* [2].

Facts about moving striations are found in *Wave Nature of Moving Striations*, written by D. A. Lee, P. Bletzinger, and A. Garscadden, [6], and in *Plasma Physics and Engineering* [2].

Often, a positive column which appears to be uniform consists in actuality of quickly moving striations. Moving striations travel from the anode to the cathode. Utilizing a high speed camera in my laboratory, I noticed moving striations look the same as stationary striations. Moving striations are a result of an oscillating polarized electric field caused by a perturbation in electron density by ion diffusion. Striations propagate as ionization waves. An illustration of this is given by Figure 2.5.4.

Perturbations of electron density, δn_e , propagate in the anode-to-cathode direction. The polarized electric field, δE , is maximum when $\delta n_e = 0$, and determines the oscillation of the total electric field. So, as δn_e propagates toward the cathode, so does δE_{max} , resulting in an oscillation of the total electric field, giving way to moving striations.

Lee, Bletzinger, and Garscadden found the velocity of striations is dependent on the pressure of the gas [5]. In *Plasma Physics and Engineering* [2], the velocity of plasma striations is derived by assuming perturbation of the electric field δE , electron density δn_e , and electron temperature δT_e change harmonically, i.e. $\propto e^{i(\omega t - k_s x)}$. From this assumption, the phase velocity of striations is derived as,

$$v_{ph} = \frac{w_s}{k_s} = \frac{1}{k_s^2 \lambda / \sqrt{\delta}} k_i n_0 \frac{\partial \ln k_i}{\partial \ln T_e}. \quad (2.5.10)$$

Simply, as a short hand, the velocity of striations is proportional to the square of the wavelength. A full derivation of the phase velocity of plasma striations is found in Section 7.4.5 of *Plasma Physics and Engineering* [2].

2.6 Sputtering, Sparking, and Arcing

Sputtering, sparking, and arcing are phenomena which occur in discharge tubes and cause difficulties in measuring the positive column striations of the glow discharge.

2.6.1 Sputtering

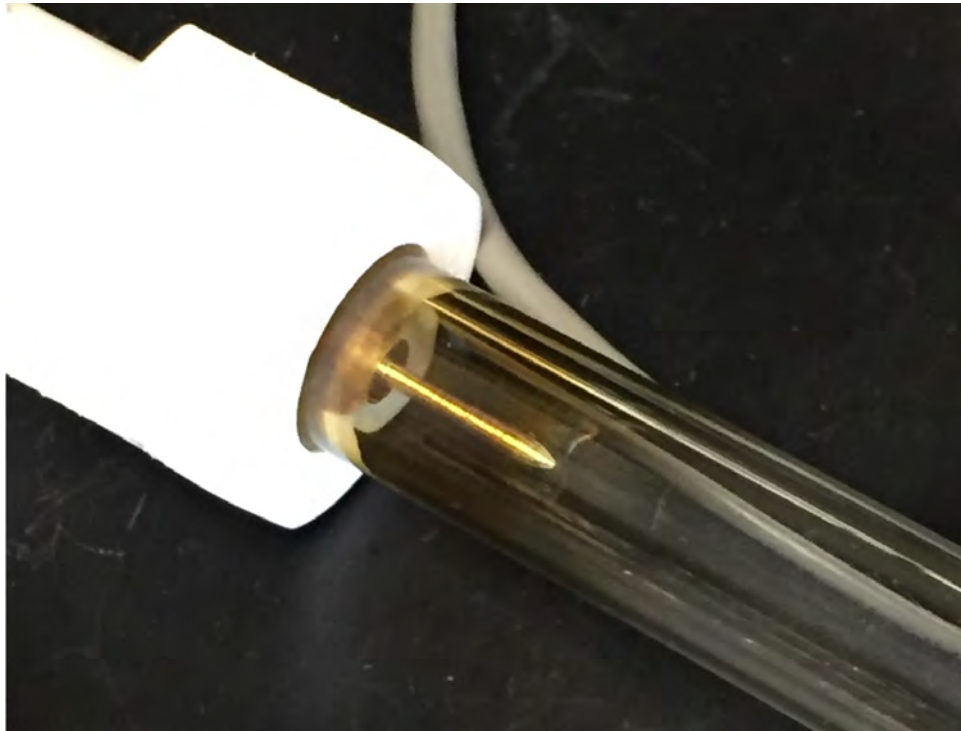


Figure 2.6.1. Image of metallic deposits on glass from sputtering.

The cathode, because it is at a low voltage, is constantly hit with positive ions while the plasma is maintained. The positive ions are much more massive than electrons. The positive ion bombardment causes a disintegration of the cathode known as sputtering. The metal that is knocked from the cathode is deposited on the walls of the cathode tube surrounding the cathode, as seen in Figure 2.6.1. As tests on the plasma continue, the glass around the cathode gradually becomes darker until the cathode is obstructed from view.

2.6.2 Sparking

Sparking is a sudden transition between non-self-sustaining discharge and self-sustaining discharge. Discharges which are not self-sustaining are dark. In a dark discharge there is a small current traveling between the anode and cathode. This current increases slightly

with an increase in voltage. The continued increase of voltage results in saturation. Saturation is when the electrons emitted from the cathode accelerate to the anode. As the voltage still continues to increase so does the current. The spark occurs once the voltage reaches a critical value V_s . At this voltage there is a transition from dark discharge to either a glowing discharge or an arc.

2.6.3 Arcing

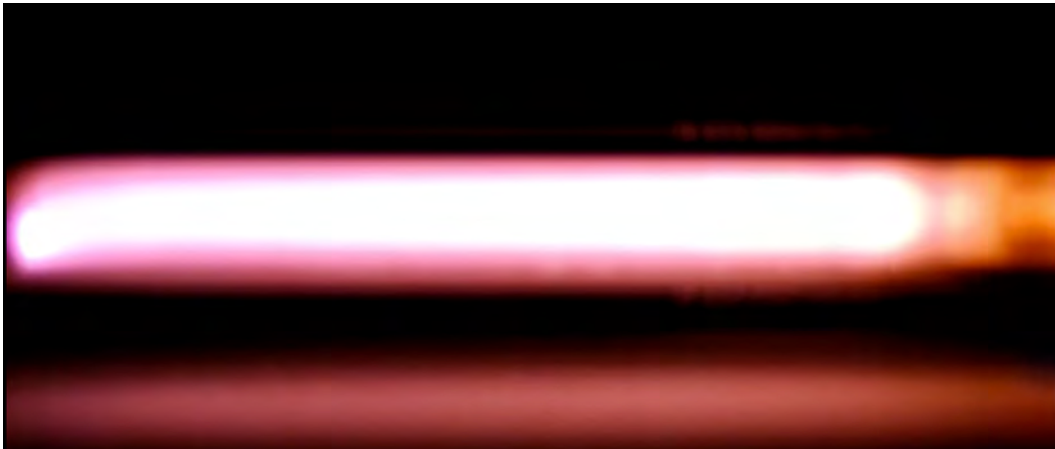


Figure 2.6.2. Arc at 500 mTorr and 1500 V

Arcing is a self-sustaining discharge which carries a high current. Arcing typically occurs during a transition from the glow discharge, which is a higher voltage discharge. The voltage drop of an arc discharge at the cathode is of the order of the minimum ionization potential of the gas. The voltage drop at the cathode causes the emission of electrons, sustaining the total discharge. An image of an arc is seen in Figure 2.6.2.

2.7 Experimental Relationships

This sections explains a number of experiments into the striated positive column from the late 19th century by Goldstein and R.S. Willows.

2.7.1 Pressure and Striation Distance

Investigations into the dependence of plasma striations on pressure were made in the late 19th century by Goldstein and R.S. Willows. Goldstein found striation distance and pressure can be related by

$$\frac{d}{d_0} = \left(\frac{p_0}{p} \right)^m. \quad (2.7.1)$$

d_0 and p_0 are the initial distance between striae and the initial pressure in which the plasma was formed. The constant m is less than one and is different for each gas used to form the plasma [4]. According to Eq. 2.7.1, the distance between striations increases as the pressure decreases.

As you can see from Figure 2.7.1, for a constant current and a constant high voltage, the distance between striations is greater for lower pressures. However, when the current increases past 90 Gal. Deflexion the relationship flips. This suggests Eq. 2.7.1 only holds true for a weak vacuum greater than 1 Torr and a high voltage.

2.7.2 Voltage, Current, and Striation Distance

The relationship between striation distance and current was investigated by R. S. Willows. Figure 2.7.2 shows for nitrogen gas, beginning at the lowest current to maintain a stable positive column, the distances between striations increase with current.

2.7.3 Electrode Shape, Tube Dimensions and Striation Distance

In Figure 2.7.1 from Section 2.7.1, one can see the shape of electrodes causes a change in the distance between striations. In this figure, electrodes used for curves A and B were wires, and the electrodes used for curve C were discs. Disc electrodes, having a much larger surface area than wires, result in more tightly packed striations. For a pressure of

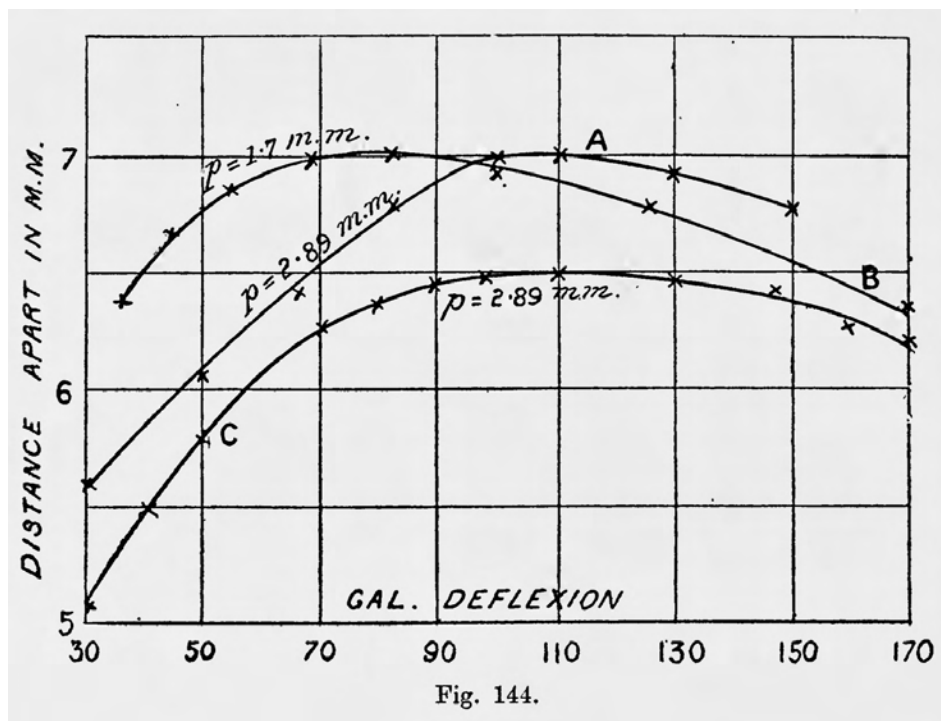


Fig. 144.

Figure 2.7.1. Distance between striations with respect to current, taken from *Conduction of Electricity Through Gases* [9].

2.89 mm Hg, the distance between striations formed from disc electrodes were around 0.25 mm shorter than those formed by wires.

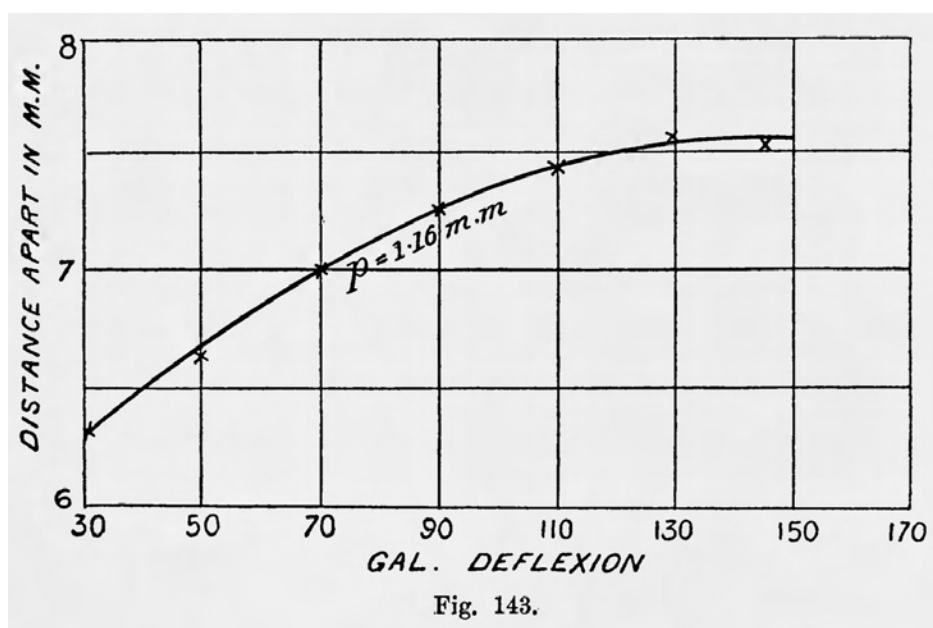


Figure 2.7.2. Distance between striations with respect to current, taken from *Conduction of Electricity Through Gases* [9].

3

Plasma Tube Design and Construction

In this Chapter, I describe the process of designing and building my plasma tube from start to finish. As is common in engineering, I went through many stages of trial and error, motivated mostly by considerations of practicality rather than designs gleamed from past apparatuses found in plasma physics literature. In designing the apparatus, I focused on maintaining a constant weak vacuum, leaking in argon gas, and altering the distance between electrodes.

3.1 Original Design

The original design of the plasma tube was made months before the building of it took place. In the process of building this tube, it became clear what would work and what would not. The first concern of designing the plasma tube was making sure it would pump down to a weak vacuum. For this, a standard rotary pump is needed to evacuate the tube to the mTorr regime.

The original design consisted of: a pyrex test tube, open at one end; one rubber plug to seal the open end of the tube; a 1 cm long metal pipe with a diameter of 0.5 centimeter; a 10-centimeters-long, 0.5 centimeter diameter, flat head steel bolt; electrical tape; epoxy; and iron wire. The tubes were purchased from McMaster-Carr.

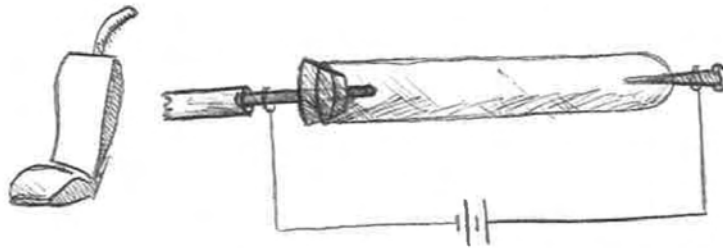


Figure 3.1.1. Schematic of the original design.

The items of this design were fairly simple. If constructed, the metal tube would enter the test tube through a hole in the rubber plug and would have been connected to a vacuum pump. The pump would bring the test tube to a low vacuum by pumping through the metal pipe, and the iron wire would wrap around the pipe and be connected to a DC voltage supply. At the other end of the test tube, the steel bolt would be encased by the closed round end by use of a blow torch, heating the pyrex to make it malleable. The bolt in this design was the cathode and the pipe was the anode.

This original design lacked much as an experimental apparatus for it would not have allowed for manipulation of any plasma parameters other than voltage and current.

3.2 Secondary Design

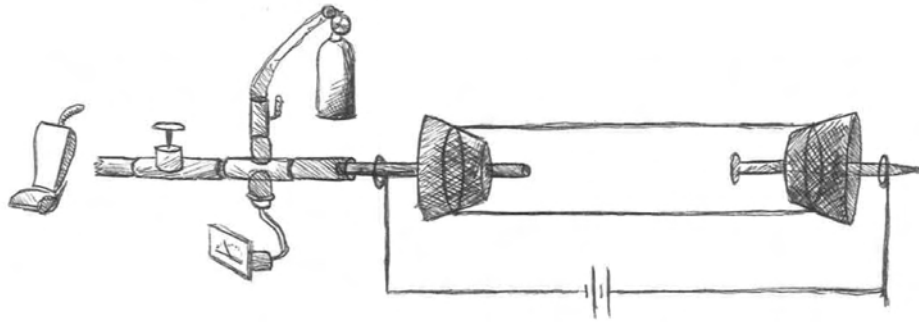


Figure 3.2.1. Schematic of the secondary design.

The second design consisted of, in order from left to right: a vacuum pump; a needle valve; a cross fitting to secure a ball valve and pressure gauge; PVC pipe; a metal rod to work as the anode; a pyrex tube open at both ends, sealed by rubber tubes; and a steel bolt to work as the cathode.

It soon became clear this design would also not work. The rubber plugs for the tube did not allow for a tight seal on the metal pipe and steel bolt. Also, the gas leak was in the wrong location and was designed to be fastened to a ball valve. For the tube to fill with the gas being leaked in, it must have been at the high pressure end of the plasma tube, and ball valves do not allow for pressure to be controlled precisely. However, with the needle valve in place, both voltage and pressure were possible parameters for manipulation.

3.3 Penultimate Design and Final Configuration

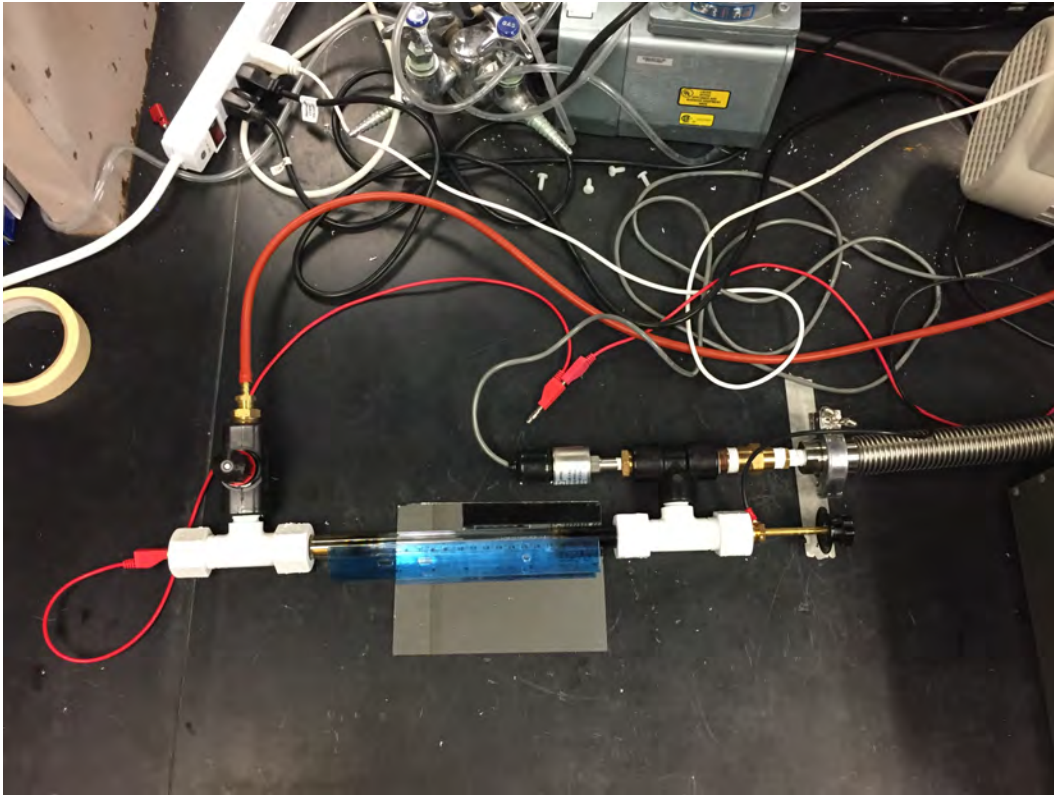


Figure 3.3.1. Photo of the apparatus used in data collection.

The second-to-last design (Figure 3.3.1) situated the gas leak and the needle valve at the high pressure end of the tube, utilizing a T-fitting. This allowed for the gas to leak into the tube through the needle valve, making it easier to control the pressure. An issue with this design was that the needle valve, which must have been manipulated by hand, was placed on the high voltage end of the tube. This posed a safety issue due to a high DC voltage being applied across the tube. The plugs for the two open ends of the pyrex tube also changed significantly. Instead of rubber plugs sealing the openings of the tube, the tube was placed into two T-fittings at each end. The opening of each T-fitting was 0.5 inches in diameter, matching the diameter of the pyrex tube. Around the tube was a nut that both fastened the tube to the connection as well as compressed an o-ring around the tube in order to prevent leaks of air into the apparatus. At the opposite ends of the

tube connection was a 1.5 inch long, 0.5 inch diameter brass plug. A 0.25 inch hole was drilled and threaded in the center of the plug for the connection of different electrodes. On the other end, a 0.25 inch hole was drilled to secure a banana plug. Banana plugs were attached on each side of the vacuum tube to supply a high DC voltage.

At the ground end of the tube, the third opening of the T-fitting connected a vacuum pump and a pressure gauge. This set-up allowed for explorations into the parameter space of the glow discharge and positive column by allowing for the manipulation of pressure, voltage, current, and gas type.

The configuration of the final apparatus used in the recording of data was the same as in Figure 3.3.1. The cathode at the right of the tube was built to move in and out of the tube without altering pressure. This electrode used a 1.5 inch long, 0.5 inch diameter brass rod with a 0.25 inch hole drilled entirely through it. Inside the rod was threading which allowed the cathode to rotate in and out of the tube, spanning a distance of 2.0 inches. The cathode maintained a seal with the rod through the compression of a 0.25 inch rubber ring.

4

Exploring Parameter Space of the Glow Discharge

In this chapter I detail my investigation into the parameter space of the positive glow discharge. Continuing off past experiments in plasma physics (see Section 2.7), I investigated the following parameters: pressure, voltage, current, shape of electrodes, type of gas, dimensions of the vacuum tube, and electrode spacing. The first order of business in this process was figuring out how to form and maintain a stable plasma. From there I was able to test each parameter to see its effect on the dimensions of the striated positive column.

4.1 Forming the Plasma

With the apparatus I constructed, the only pressure regime in which I was able to form a plasma was between 200 and 500 mTorr. The vacuum pump available to me could evacuate at most a volume down to 50 mTorr. When attached to my vacuum tube, due to its size and assembly, the pump could evacuate the space to a minimum of 200 mTorr. This constrained my investigation to plasmas formed above 200 mTorr, excluding phenomena (10) - (16) detailed in fig. 2.5.1.

Forming a stable plasma required evacuating the tube down to 200 mTorr. I used a thermocouple pressure gauge to determine if the pressure was stable. Once the needle of

the pressure gauge stayed at rest, the voltage generator was turned on. This DC voltage generator turns on at 500 V. The voltage can be increased using three different nob by 1, 50, or 500 V at a time. I ramped up voltage by 100 V at a time. In both air and argon gas, the plasma ignites around 1000 V. At this point, I was able to increase the voltage or decrease the voltage while maintaining a stable plasma. After the plasma is ignited at the breakdown voltage, typically 1000 V, the voltage can be decreased to about 800 V before it disappears. I was not able to test voltages over 2000 V because it caused the power supply to blow a fuse.

After maintaining a stable plasma at 200 mTorr and 1000 V, the pressure was increased by loosening the nob of a needle valve. When the nob is turned, a needle lifts out of a hole in the valve, allowing a small amount of air or gas back into the tube. The pressure regime of which I was able to work was constrained between 200 and 500 mTorr due to sparking. As the pressure increased above 500 mTorr, the anode and cathode began to arc. As the voltage continued to increase, the arcing became more rapid. Each arc sends a surge of current through the voltage generator, resulting in a blown fuse and the loss of the plasma. This limited my investigation into higher pressure phenomena like (1) - (7) detailed in Figure 2.5.1.

Within these limitations, I explored the parameter space in the manner presented below. In the following Chapter 5, I describe my experimental setup and measurement techniques, present my data, followed by an analysis, and conclude my project with further research and experimental avenues to pursue.

4.2 Manipulating Parameter Space of Weak Vacuum Plasma

4.2.1 *Changing Pressure*

On the high voltage end of the tube a needle valve was installed. This needle valve was used to manipulate the pressure inside the tube and allow for the testing of other gases by leaking said gas into the tube. The pressure regime that gave the best results for forming

a striated positive column was found to be around 200 mTorr. In manipulations of the pressure with the needle valve, only slight turns of the nob caused the pressure to increase by nearly 300 mTorr. Around 400 mTorr, according to Eq. 2.7.1, I should have seen the distance between striations of the positive column change by a factor of 2. This change in striation distance was not seen. According to *Conduction of Electricity Through Gases* [9], the pressure regime at which Goldstein made his discovery was around 1 Torr [4] which was out of the pressure range I could test. It seems this relation does not hold between 200 and 400 mTorr.

If a striated positive column forms at 200 mTorr with a given voltage, at 500 mTorr with the same voltage, the plasma takes on a very different form. The positive column, Crookes dark space, cathode glow, etc. are not seen at this pressure regime. Instead, to the naked eye, the whole tube illuminates into one bright flash of light repeatedly. What is seen is an electrical arc between the anode and cathode. As the pressure in the tube increases, so does the number of atoms of gas in which the electric field interacts. At this slightly higher pressure the number of atoms increase to a point of high conductivity. With each flash, the current through the gas spikes. At higher pressures the arcing occurs more rapidly than at lower pressures. On numerous occasions, the frequency of these spikes in current became so rapid the fuse in the voltage generator blew. To read more about sparking and arcing see section 2.6.

At higher pressures of gas a few differences were noticed between the same gas at lower pressures. Primarily, the voltage required to ignite the plasma, also known as the breakdown voltage 2.2.1, is lower than the voltage it takes to ignite a plasma at lower pressure. The reason for this becomes clear when the electron avalanche is understood. In one experiment with argon gas, the voltage required to cause an electron avalanche at 500 mTorr was 200 V less than that required at 200 mTorr.

With the aid of a high speed camera, I found that between these moments of intense sparks of light, at pressures above 500 mTorr, there were striations moving from the anode

to the cathode. To read more about moving striations see section 2.5.3. However, even with the ability to see the dynamics of this flashing plasma anywhere from 200 frames-per-second to 10,000 frames-per-second, it became clear the resolution in which the pressure could be manipulated was much too low. It was not possible to see the subtle changes in striation distances when the pressure can only be altered at increments of 300 mTorr and at a pressure regime outside that of Goldstein's.

4.2.2 Voltage and Current

In the way my apparatus was designed, I did not have direct control over the current. I did, however, have control over the voltage. As the voltage increased, the current would decrease. An ammeter was placed in series with the plasma tube to monitor the current. I used the ammeter to monitor the current in order to keep the voltage supply from exceeding its power limit of 60 W.

I found, while exploring the effect of voltage on the glow discharge, at higher voltages, the positive column and cathode glow intensified in light. The striations of the positive column became sharper at higher voltages and were easier to see. The distances between striations were easier to measure at higher voltage. However, contrary to figure. 2.7.2, the distance between striae did not decrease with the increase of voltage. As the voltage increased, the striations simply stayed in the same place, growing in brightness. My exploration into the effect of increased voltage was constrained by the upper limit allowed by the voltage generator I utilized. Again, my plasma tube did not form plasma in the same pressure regime as Willows'; therefore, I decided its experimental functionality would not directly use voltage and current.

4.2.3 Shape of Electrode

I decided that a main topic of inquiry would be the shape of the anode and cathode because of the experiment detailed in 2.7.1. Although Willows was testing the effect of current, voltage and pressure on striation distance, he also noticed a difference between

that relationship with respect to electrode shape; the distances between striations with wire electrodes were greater than those distances for disc electrodes.

The first formations of the plasma used quarter-inch, flat ended, brass rods as the electrodes. In creating plasma, these worked perfectly well. Typically the plasma would ignite around 1000 V with the pressure maintained around 200 mTorr. To see if the plasma would form at a lower breakdown voltage, and to see if this would alter the striated positive column, pointed electrodes were machined. The hypothesis was, pointed electrodes would form a higher electric field within the tube, for a given voltage, due to higher concentration of charge at the pointed tip.

There were few differences in plasma between the two shapes of electrodes. I therefore decided not to focus on a detailed examination of how electrode shape effects plasmas. Both shapes resulted in a breakdown voltage of about 1000 V. Also, with both electrodes, after ignition, the voltage across the plasma could still only be lowered to around 800 V before it disappeared. The most important difference between the flat and pointed electrodes was that the pointed electrodes seemed more predisposed to arcing and sputtering (see section 2.6). Arcing often occurred during examinations of the striated positive with both electrodes. At 200 mTorr, when the arc would occur, there would be a flash of bright light and a small blue mark at which the arc seemingly hit the cathode. After the arc, the positive column would reappear just as it was a moment before. Arcing appeared to cause an increase in sputtering which in turn causes a fogging of the inside of the tube. This fogging is a build up of thin layers of brass, evaporated from the cathode. With a sputtering electrode, it becomes increasingly more difficult to see the plasma. For this reason, flat-end electrodes seemed the most reasonable shape.

4.2.4 *Type of Gas*

Research into the nature of plasma with respect to the gas in which it is formed was common during the early 20th century. Experimenting with different gases was also of interest in this exploration. Noble gases are benign in their interactions with the human

body if inhaled and serve to form stable plasmas, making them the best species to use in a plasma chamber. It is easy to form a plasma with a noble gas because it takes a relatively low amount of energy to ionize them. The voltage required to knock an electron away from an atom of argon, leading to the needed chain reaction for an electron avalanche, is less than that for a non-noble gas (see figure 2.2.3).

In this study, argon gas was leaked into the vacuum tube using a needle valve. It is important to, before igniting the plasma, purge the tube of air. In the initial run through using argon gas, the tube had not been purged. This caused the positive column to alternate between bright orange and salmon pink. The positive column in air is pink, and it seemed as though the voltage across the tube was igniting plasma made of argon and plasma made of air. This problem went away after purging the tube before each test. The process of purging the tube is: fill the tube with argon through the leak valve, pump it down to a weak vacuum, leak more argon gas into the tube (raising the pressure), pump that down to a weak vacuum, and repeat. This needs to be done several times to make sure the air is in small concentration.

Although giving a different color of plasma, the argon gas had similar breakdown voltages and striation spacing as the plasma in air.

4.2.5 *External Magnetic Field*

External magnetic fields have a great effect on the positive column of the glow discharge. Using a simple bar magnet, I was able to control the length of the positive column by placing either the positive or negative end of the magnet next to the cathode end of the column. Moving the bar magnet down the tube towards the cathode extended the positive column as if I were attracting a piece of metal; this is shown in Figure 4.2.1. As the positive column would extend, the striations moved along with it, staying the same distance apart. This process produced more striations to fill in the gap left by the extension of the positive column. This looked as if I were pulling striations out of the anode. This same process with the opposite orientation of the magnet cause the same



Figure 4.2.1. Illustration of how an external magnetic field extends the positive column.

result. Interestingly, extending the positive column to within a couple centimeters of the cathode often made the plasma disappear.

I was able to change the distance of striations by placing one end of the bar magnetic above the center of the positive column. This did not increase the length of the positive column but seemed to expel the striations below the magnetic outwards, causing the striations to become more tightly packed at the anode and cathode end and loosely packed in the center.

Although very effective at changing the spacing of the striated positive column, the bar magnet was not easily and accurately controlled and did not provide an adequately uniform magnetic field for experimentation. In future studies I could see using a current loop or Helmholtz Coils around the center of the tube to form a relatively uniform and manageable magnetic field for testing.

4.2.6 *Electrode Spacing and Tube Dimensions*

I first began exploring the effect of electrode spacing in the following manner. I observed the positive column at a voltage V and pressure P with a electrode separation of l_0 . I turned on the voltage supply and vacuum pump, detached the cathode from its T-fitting, and removed it from the apparatus. The cathode I designed was threaded at one end and screwed into a brass cylinder plug. Because of the threading, I was able to screw the cathode out of the plug by nearly 1.5 cm while still attached to the plug. I then reconnected everything, turned the pump and voltage supply on again, established a plasma, and returned the voltage and pressure back to V and P , but now with an electrode spacing of l . It was immediately apparent that the decrease I made in electrode spacing caused a decrease in the length of the positive column. After this discovery, not only was I motivated to test the effects of electrode spacing further, I also became interested in altering the dimensions of the tube itself.

An investigation into the effect of tube diameter on striation spacing was conducted by Willows and detailed in section 2.7.3 of this paper. Experimenting with different diameters of my plasma tube did not seem practical because of the nature in which I attached the tubes to the rest of the apparatus. For my design, it made much more sense to vary the length of the plasma tube. In a sense, varying the length of the tube merely changed the distance between anode and cathode. In one exploration, maintaining the same voltage and pressure, I attached a tube 4 inches longer than my original. This caused a plasma to form with a much longer positive column than before.

After these explorations into the parameters of the glow discharge, it became clear the most manageable and illuminating parameter to alter was the distance between electrodes. The next and final chapter presents the data, analysis, and conclusion of my project.

5

Data Collection and Analysis

5.1 Experimental Set-Up and Measurement Techniques

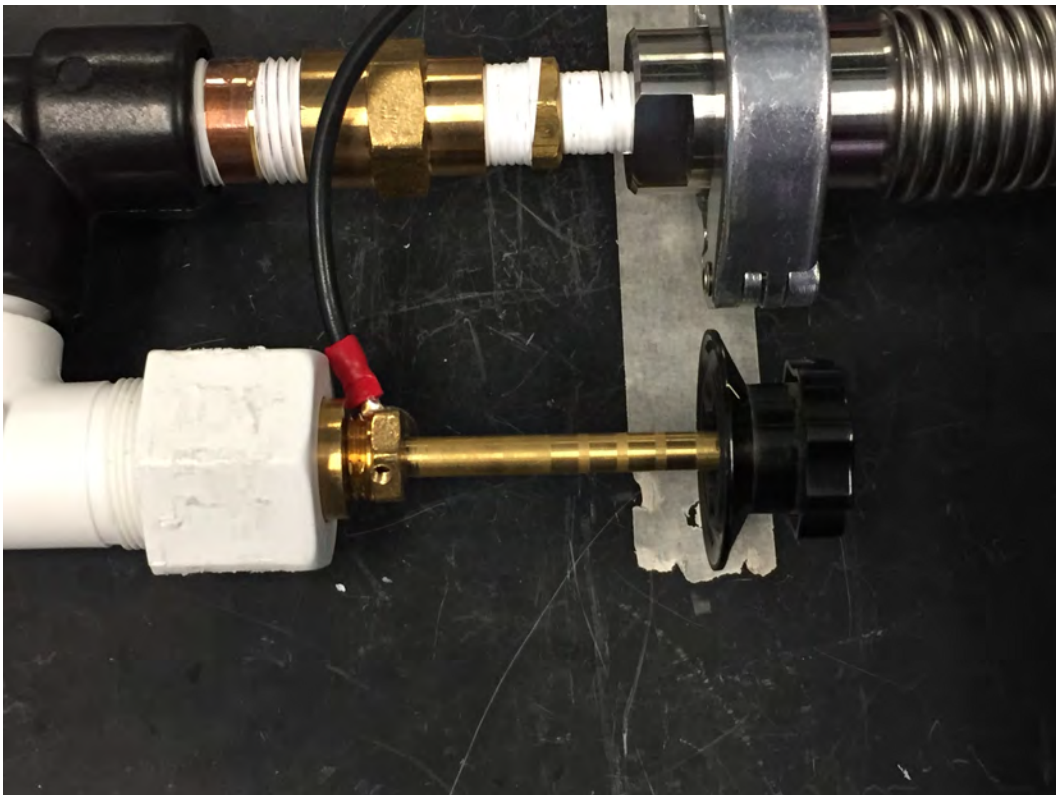


Figure 5.1.1. Moveable cathode attached to plasma tube.

In this experiment I measured the length of the positive column and the length of the positive column striations both with respect to distance between anode and cathode. Measurements were taken in air and argon gas. The experiment conducted used the final design of Section 3.3. My apparatus consisted of three interchangeable glass tubes. The tube lengths were 8, 10, and 12 inches. The moveable cathode was able to alter the electrode distance by 1 cm; an image of this cathode is seen in Figure. 5.1.1. Using the three tubes and the moveable cathode resulted in cathode length ranging a total of 10 cm. As will be seen in the following section, this range is broken into three electrode length groups with gaps of 4 cm.

Each measurement was taken in electrode distance increments of 0.1 cm, corresponding to one full rotation of the cathode. Due to an error in machining the cathode, it was not perfectly centered in the tube but offset from the center by a small angle. The position of the cathode for which I decided to take data was the most centered position. A 180° rotation of the cathode from its most centered position was the least centered position, nearly 2 mm from the wall of the tube. This position caused a much longer positive column than what was seen at the most centered position in both air and argon. As was discussed in Section 2.5.2, the net negative charge deposited on the surface of the plasma tube determines the shape of the striations. This may be why when the cathode is angled closest to the wall of the plasma tube the positive column is maximized. It was clear in the collecting of data that this oscillation in column length from 0° to 360° , maximum at 180° and minimum at 360° , was not due to an increase in length; it is highly unlikely the length of the positive column would make exactly one full oscillation with one full rotation of the cathode. The error in the cathode position required data to be taken with respect to the same orientation as to be sure the length changes of the positive column were due only to the change in distance between the anode and cathode.

In order to accurately measure the length of the positive column, the length of the striations, and the distance between electrodes, a mirror was placed under the plasma

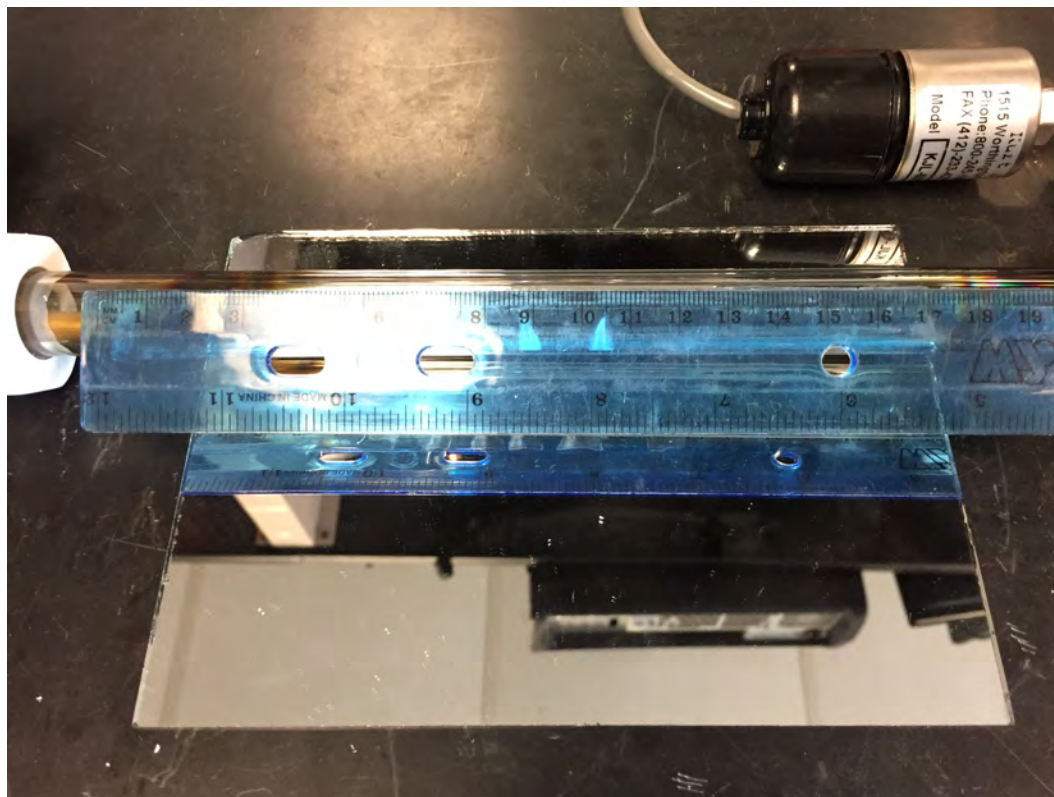


Figure 5.1.2. Ruler, tube, and mirror set up.

tube, as seen in Figure 5.1.2. The mirror was used to mitigate issues of parallax. When measuring the position of an electrode or the edge of a striation, the mirror was used to make sure I was looking directly at the object, making a 90° angle between my line of sight and the plane of the mirror. This is visualized in Figure 5.1.3; in the recording of object positions I closed one eye and moved my head back and forth until the object I saw and the reflection of that object were directly inline with one another. This process was done every time I measured the distance between electrodes and the length of the positive column and striations.

The pressure was controlled using a needle valve for both air and argon gas. For air, the needle valve was free to let lab air into the tube. For argon, the needle valve was attached to a tank of argon gas via a rubber tube. To allow in air, the orange tube seen in Figure 5.1.4 was simply removed from its brass connection. Turning the needle counterclockwise

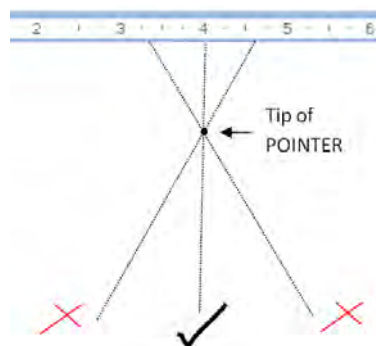


Figure 5.1.3. Pictorial explanation of parallax [16].

increased the pressure in the tube, allowing in more of either species, while turning it clockwise decreased the pressure.

The length of striations were measured from the curved crest of one striation to the beginning of another striation, displayed in Figure 5.1.5. The length of the positive column was measured from the crest of the first striation on the cathode side of the positive column to the tip of the anode.

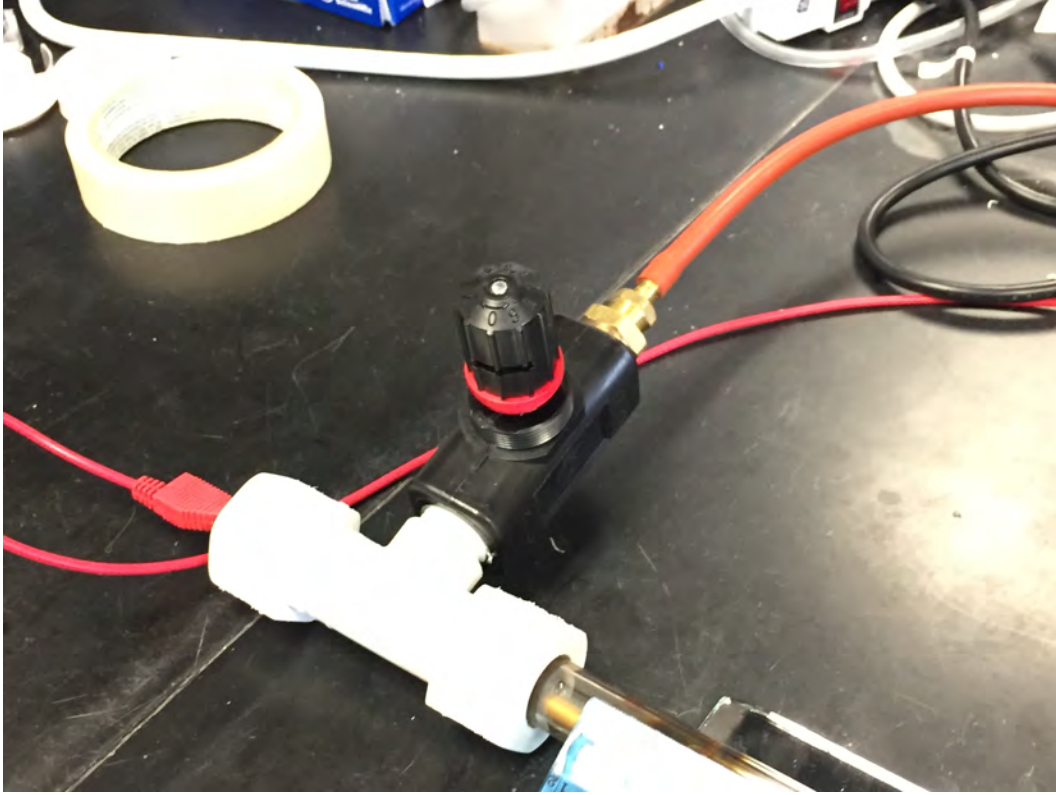


Figure 5.1.4. Needle valve allowing in argon gas.

5.2 Data and Analysis

The dependence between electrode spacing and striation length was measured over a range of 10 cm for both air and argon gas. These measurements were taken while maintaining a constant voltage of 1.5 kV and a pressure of 250 mTorr. Likewise, the dependence between electrode spacing and positive column length was also measured over a range of 10 cm. and the voltage and pressure held constant on 1.5 kV and 250 mTorr.

The data taken for striation length with respect to electrode spacing is plotted in Figure 5.2.1, labeled with stars and circles. It is clear the distance between electrodes has a minimal effect on the length of the striations. For a plasma of air, the length of striations roughly held constant around 1.4 cm as the electrodes were moved closer together. Similarly, the length of the striations in argon gas stayed around 1.0 cm. This

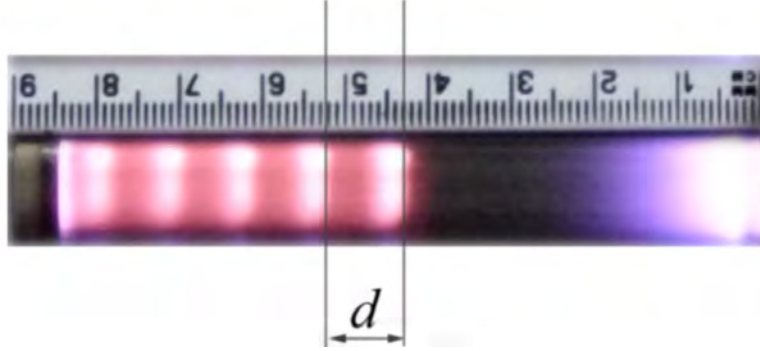


Figure 5.1.5. Measurement length of one striation, taken from [13].

shows that the patterns of the positive column are not caused by electrode boundaries, further divorcing plasma striations from standing wave phenomena.

The length of the positive column depends linearly on the distance between electrodes in air and argon gas. As seen in Figure 5.2.1, as the distance between anode and cathode increases, the length of the positive column increases as well.

The length of the positive column in argon follows a linear fit of,

$$l_{\text{argon}} = 1.02L - 3.74 \text{ cm.} \quad (5.2.1)$$

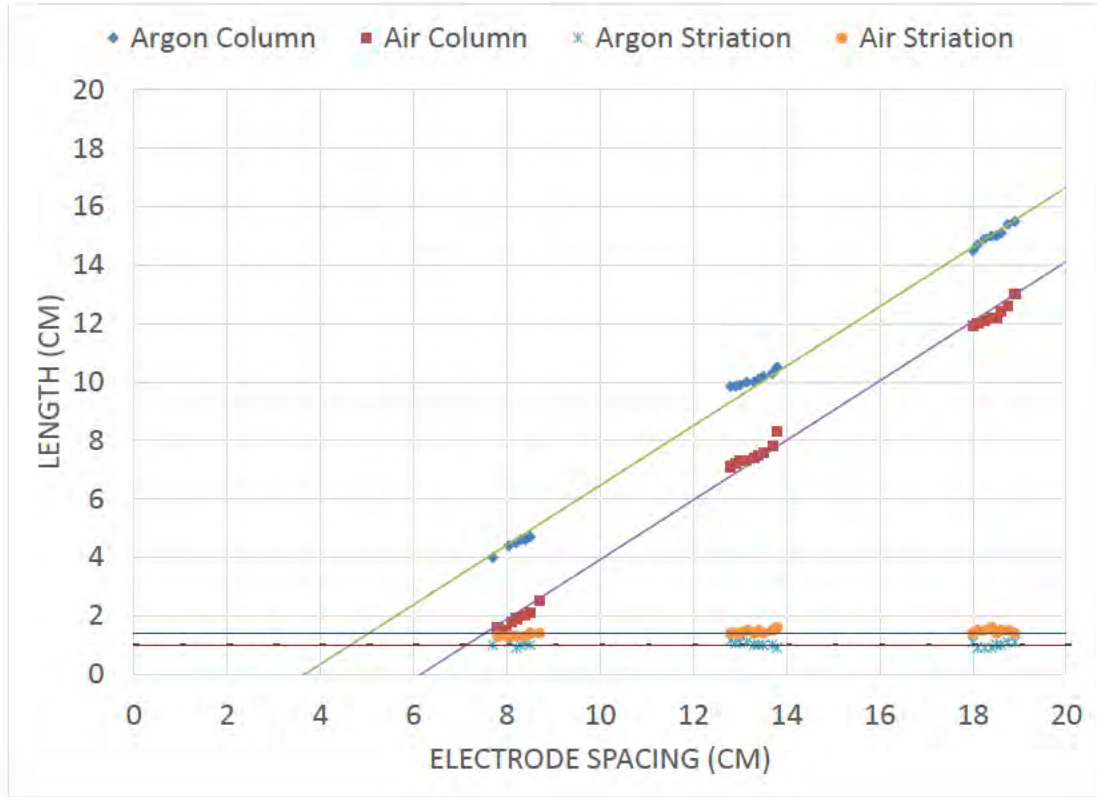


Figure 5.2.1. Plot of column and striation length vs electrode spacing. The two lines intersecting the horizontal-axis are the best fit for column length vs electrode spacing for air and argon. The two horizontal lines correspond to the average striation length for air and argon.

In this equation l_{argon} is the length of the positive column in argon and L is the distance between electrodes. This equation suggests that the positive column cannot be maintained for electrode spacing less than 3.67 cm in argon gas. Likewise, the length of the positive column in air trends as,

$$l_{air} = 1.02L - 6.28 \text{ cm.} \quad (5.2.2)$$

As above, l_{air} is the length of the positive column in air. The positive column in air should disappear at an electrode spacing of 6.16 cm. However, there seems to be a minimum length of the positive column. In altering the length of the positive column with a bar magnet (see

Section 4.2.5) the positive column can only be shortened to a minimum length. Possibly a glow discharge cannot form at these minimum electrode spacings because the positive column is necessary for maintaining a stable plasma. The other positive glow areas never appear without the appearance of the positive column.

The slopes of Eqs. 5.2.1 and 5.2.2 are dimensionless and nearly equal to 1. The length of the positive column depends directly on electrode distance, but the length of striations does not. This is also seen when altering the length of the positive column with a bar magnet (see Section 4.2.5). When extending the positive column in the direction of the cathode, striations seem to be pulled out of the anode with constant length. I think this fact is due to the negative charge distribution determining the shape of the striations (see Section 2.5.2); Nedospasov states in *Striations* that striations are formed in the positive column [5]. The diffusion of electrons to the wall of the tube happens within the positive column. If the diffusion of positive ions and electrons is the same in the positive column regardless of length, it makes sense the striations would maintain a constant length.

In argon gas, the length of the positive column is nearly 2.5 cm longer than the positive column in air. Also, the length of argon striations is about 0.4 cm shorter than striations in air. Therefore, the positive column in argon is longer, more tightly striated, and maintained at closer electrode distances than in air. This may be because the voltage required to ionize argon is less than the voltage needed to ionize air (see Section 2.2.1). For a constant voltage and pressure, the voltage drop across argon can endow the positive and negative ions with more kinetic energy than the same voltage drop could for air. It is seen that when voltage increases the length of the positive column also increases. It's possible the higher the kinetic energy of the ions results in a longer positive column. For the same voltage, argon ions in a glow discharge have a higher greater energy than air ions.

It isn't exactly clear why argon striations are shorter than air striations. Eq. 2.5.9 found in Section 2.5.2 states the length of a stationary striation depends on the ratio between

the electron diffusion coefficient D_e and the ambipolar diffusion coefficient D_a :

$$l = \frac{a}{\beta} \ln \left[1 + \frac{D_e I}{D_a i} \right].$$

a and β were equal for air and argon in the experiment because they depend only on the dimensions of the tube. Due to voltage, current, and pressure being held constant, I and i were also the same in each case. This mean, since argon striations are closer than air striations, the ratio between D_e and D_a is less in argon than it is in air.

5.3 Further Studies

First of all, measurements should be taken with electrode spacings of 3.67 cm and 6.16 cm in argon and air respectively to determine if in fact the positive column does not appear. Unfortunately, due to the shortest tube being 8 inches and the moveable cathode ranging only 10 cm, I was not able to test this prediction. But the primary goal of this research was to test the impact of electrode spacing on the patterns seen in plasma.

The analogy between standing pressure waves and the striated positive column led me to think the anode and cathode played an important role; however, this is not true. But it may still be the case that boundary conditions of the tube similarly cause the patterns seen. The curved shape of striations is caused by a net negative charge depositing on the walls of the glass tube. Directly manipulating the diameter of the plasma tube may lead to a better understanding of what causes these patterns.

Moreover, mandala-like patterns can be seen on circular drum heads due to classical standing waves. Constructing a two-dimensional plasma tube, analogous to a drum-head, could show how similar these two phenomena really are; if the patterns in a two-dimensional positive column resemble those on a drumhead, this analogy may be worth pursuing. Similar to the experiment conducted in this study and the one suggested above, the two-dimensional plasma tube could be designed to allow the radius of the drumhead-like tube and the electrode distance to be adjusted.

Bibliography

- [1] James Cobine, *Gaseous Conductors*, Dover Publications, Inc, New York, NY, 1958.
- [2] Alexander Friedman and Lawrence Kennedy, *Plasma Physics and Engineering Second Edition*, CRC Press, Boca Raton, FL, 2011.
- [3] F. Reif, *Fundamentals of Statistical and Thermal Physics*, Waveland Press, Inc., Long Grove, Illinois, 1965.
- [4] Wied Goldstein, *Schichtabstand und Schichtpotentialdifferenz in der positiven Glimmentladung; von Friedrich Wehner*, Annalen der Physik **xv** (1900), 277.
- [5] A. V. Nedospasov, *Striations*, Soviet Physics Uspekhi **11** (1968), 174 – 187.
- [6] D. A. Lee, P. Beltzinger, and A. Garscadden, *Wave Nature of Moving Striations*, Journal of Applied Physics **37** (1966), 377.
- [7] Jacob Millman, *Vacuum-tube and Semiconductor Electronics*, McGraw-Hill Book Company, York, PA, 1958.
- [8] Andrew Guthrie, *Vacuum Technology*, John Wiley and Sons, 1963.
- [9] J. J. Thomson, *Conduction of Electricity Through Gases*, Cambridge: Printed by J. and C. F. Clay, at the University Press, 1903.
- [10] *Gaseous Dielectrics*, <http://nptel.ac.in/courses/108104048/lecture5/slide1.htm>.
- [11] H H Wittenberg, *Gas Tube Design*, http://www.g3ynh.info/disch_tube/Wittenberg_gas_tubes.pdf.
- [12] *Gas Discharge Tubes*, http://www.g3ynh.info/disch_tube/intro.html.
- [13] V A Lisovskiy, V A Koval, E P Artushenko, and V D Yegorenkov, *Validating the Goldstein-Wehner law for the stratified positive column of dc discharge in an undergraduate laboratory*, European Journal of Physics **33** (2012), 1537-1545.
- [14] The University of Michigan Physics Department, *3D30.60 - Kundt's Tube*, <https://sharepoint.umich.edu>.

- [15] Nancy Huang and Ivy Ngo, *Evolution of the Atomic Model*, <http://evolutionoftheatomicmodel.weebly.com/rutherford-bohr-model.html>.
- [16] Wikipedia The Free Encyclopedia, *Parallax*, <https://en.wikipedia.org/wiki/Parallax>.